
Networked Communication for Decentralised Agents in Mean-Field Games

Patrick Benjamin

Department of Computer Science
University of Oxford
Oxford, UK OX1 2JD
patrick.benjamin@jesus.ox.ac.uk

Alessandro Abate

Department of Computer Science
University of Oxford
Oxford, UK OX1 2JD
alessandro.abate@cs.ox.ac.uk

Abstract

We introduce networked communication to the mean-field game framework. In particular, we look at oracle-free settings where N decentralised agents learn along a single, non-episodic evolution path of the empirical system, such as we may encounter for a large range of many-agent cooperation problems in the real-world. We provide theoretical evidence that by spreading improved policies through the network in a decentralised fashion, our sample guarantees are upper-bounded by those of the purely independent-learning case. Moreover, we show empirically that our networked method can give faster convergence in practice, while removing the reliance on a centralised controller. We also demonstrate that our decentralised communication architecture brings significant benefits over both the centralised and independent alternatives in terms of robustness and flexibility to unexpected learning failures and changes in population size. For comparison purposes with our new architecture, we modify recent algorithms for the centralised and independent cases to make their practical convergence feasible: while contributing the first empirical demonstrations of these algorithms in our setting of N agents learning along a single system evolution with only local state observability, we additionally display the empirical benefits of our new, networked approach.

1 Introduction

Multi-agent reinforcement learning (MARL) [1; 2] is a generalisation of reinforcement learning [3] that has recently seen empirical success in a variety of domains, underpinned by breakthroughs in deep learning, including robotics [4–6], autonomous driving and infrastructure [7; 8], games [9–11], social science / cooperative AI [12–15] and economics [16; 17]. However, it has usually been computationally difficult to scale MARL systems beyond those with agents numbering in the low tens, as the joint state and action spaces grow exponentially with the number of agents [17–23]. Nevertheless, the value of reasoning about the cooperation among very large populations of agents has been recognised, and a distinction is sometimes drawn between multi- and many-agent systems [24–26]. The latter situation is often more useful (as in cases where better solutions arise from the presence of more agents [6; 27; 28]), more fault tolerant [29], or otherwise more reflective of certain real-world systems, such as financial markets [16; 17; 30], cryptocurrency mining [31], smart infrastructures with large populations of autonomous vehicles [32–34], cloud resource management [35], smart grids, and other large-scale cyber-physical systems [36; 37].

The mean-field game (MFG) framework [38; 39] seeks to tackle the scalability issue for such applications by modelling a representative agent as interacting not with the other individuals in the population on a per-agent basis, but instead with a distribution of other agents, known as the *mean field*. Related to similar concepts in statistical physics [40], the mean-field framework analyses the limiting case when the population consists of an infinite number of symmetric and anonymous agents,

that is, their reward and transition functions are identical to each other’s and depend on the mean-field distribution rather than on specific other players. In this work we focus on MFGs with stationary population distributions (a.k.a. stationary MFGs) [21; 41–43], for which the solution concept is the mean-field equilibrium (MFE), which reflects the situation when the agents respond optimally to the population distribution that arises when all other agents follow that same optimal behaviour. The MFE can be used as an approximation for the Nash equilibrium in a finite-agent game, with the error in the solution reducing as the number of agents N tends to infinity [41; 44].

For large, complex real-world many-agent systems, it may not be feasible to find MFEs analytically or via oracles/simulations of an infinite population [19–21; 35; 41; 42; 45–60], such that learning must be conducted directly by the agents in their deployed environment. In such settings, desirable qualities for mean-field algorithms include: learning from the empirical distribution of N agents without generation or manipulation of this distribution by the algorithm itself or by an external oracle; learning from a single continued system evolution (also referred to in other works as a single sample path/trajectory [42; 43]); model-free learning; decentralisation; good theoretical sample complexity for convergence to the Nash equilibrium; fast practical convergence; and robustness to unexpected failures of decentralised learners or changes in the size of the population [61]. However, methods for finding equilibria in this previously largely theoretical framework have traditionally relied on assumptions that may be too strong in real-world applications [19; 20; 39; 41; 45; 51; 52; 62–67]; see Appendix A for an extended discussion of this related work. In particular, almost all prior work relies on a centralised controller to orchestrate the learning of all agents [21; 41; 42; 45; 68]. Outside of MFGs, the multi-agent systems community has recognised that the existence of a central controller is a very strong assumption, as well as one that can both restrict scalability by constituting a bottleneck for computation and communication, and reveal a single point of failure for the whole system when applied to real-world problems [2; 69–72]. For example, if the single server coordinating all the autonomous vehicles in a smart city were to crash, the entire road network would cease to operate. More recent work has explored MFG algorithms for independent learning with N agents [43; 60; 73; 74]. However, prior works generally focus more on theoretical sample guarantees than the speed of practical convergence, and have not considered robustness in the sense we address (Appendix A [36; 75]), despite fault-tolerance being one of the original motivations behind many-agent systems.

We address *all* of these desiderata by introducing a communication network to the mean-field setting, to the best of our knowledge for the first time. Communication networks have seen success in other works on multi-agent settings, attempting to remove the reliance on centralised structures [70–72; 76–82]. We provide two versions of our algorithm for mean-field learning with networked agents from a continued system evolution, by which agents approach policy consensus after decentralised updates by adopting policies broadcast to them by neighbours. Firstly, an ‘idealised’ version of the algorithm (Algorithm 1, Section 3.2) which allows us to analyse the theoretical sample guarantees of our architecture in comparison with those provided for the centralised and independent algorithms in Yardim et al. [43, Algorithms 2 and 3], of which ours is a generalisation (see Section 3.4). The sample guarantees of their independent algorithm can be significantly worse than in the centralised case [43]; we show that the sample complexity of our networked algorithm is upper bounded by that of the independent case but is likely to outperform it. Secondly, we present a modified version of the networked algorithm (Section 3.5) that makes it possible to converge in a practical time (we do not update its theoretical analysis). We similarly modify the centralised and independent algorithms from Yardim et al. [43], the original versions of which we found to take too long to converge in practice (Yardim et al. [43] provides no empirical demonstrations of their algorithms, such that our empirical results of mean-field learning with N agents and local state observability from a single system evolution *in the centralised and independent settings*, are also novel contributions in themselves). On this basis, we conduct numerical comparisons of the three architectures, demonstrating the benefits of communication for both system robustness and convergence speed (Section 4). For further discussion of how networked communication can benefit robustness in large cooperative systems, and background to our experimental settings, see Appendix B.

Societal impact and harmful consequences. As with many advances in machine learning, and those relating to multi-agent systems in particular, in the long term this avenue of research could have negative social outcomes if pursued by malicious actors, including surveillance and military uses. However, it also has a large range of potential beneficial applications (such as smart grids and disaster response), and in any case, our work is primarily foundational and far from deployments. Moreover,

better understanding the dynamics of large multi-agent systems (as we seek to do in this paper) can contribute to ensuring safety by reducing the possibility of unexpected failures.

2 Preliminaries

N denotes the number of agents in a population, with \mathcal{S} and \mathcal{A} representing the finite state and common action spaces, respectively. The set of probability measures on a finite set \mathcal{X} is denoted $\Delta_{\mathcal{X}}$, and $\mathbf{e}_x \in \Delta_{\mathcal{X}}$ for $x \in \mathcal{X}$ is a one-hot vector with only the entry corresponding to x set to 1, and all others set to 0. For time $t \geq 0$, $\hat{\mu}_t = \frac{1}{N} \sum_{i=1}^N \sum_{s \in \mathcal{S}} \mathbb{1}_{s^i=s} \mathbf{e}_s \in \Delta_{\mathcal{S}}$ is a vector denoting the empirical state distribution of the N agents at time t . The set of policies is $\Pi = \{\pi : \mathcal{S} \rightarrow \Delta_{\mathcal{A}}\}$, and the set of state-action value functions (Q-functions) is denoted $\mathcal{Q} = \{Q : \mathcal{S} \times \mathcal{A} \rightarrow \mathbb{R}\}$. Function $h : \Delta_{\mathcal{A}} \rightarrow \mathbb{R}_{\geq 0}$ denotes a strongly concave function, which in our experiments is the scaled entropy regulariser $\lambda h_{ent}(u) = -\lambda \sum_a u(a) \log u(a)$, for $a \in \mathcal{A}$, $u \in \Delta_{\mathcal{A}}$ and $\lambda > 0$ (the choice of λ is discussed in Appendix F.4).

Definition 2.1 (N -player symmetric anonymous games). An N -player stochastic game with symmetric, anonymous agents is given by the tuple $(N, \mathcal{S}, \mathcal{A}, P, R, \gamma)$, where \mathcal{A} is the action space, identical for each agent; \mathcal{S} is the identical state space of each agent, such that their initial states are $\{s_0^i\}_{i=1}^N \in \mathcal{S}^N$ and their policies are $\{\pi^i\}_{i=1}^N \in \Pi^N$. $P : \mathcal{S} \times \mathcal{A} \times \Delta_{\mathcal{S}} \rightarrow \Delta_{\mathcal{S}}$ is the transition function and $R : \mathcal{S} \times \mathcal{A} \times \Delta_{\mathcal{S}} \rightarrow [0,1]$ is the reward function, which map each agent's local state and action and the population's empirical distribution to transition probabilities and bounded rewards, respectively, so that

$$s_{t+1}^i \sim P(\cdot | s_t^i, a_t^i, \hat{\mu}_t), \quad r_t^i = R(s_t^i, a_t^i, \hat{\mu}_t), \quad \forall i = 1, \dots, N. \quad \square$$

The policy of an agent is given by $a_t^i \sim \pi^i(s_t^i)$, that is, it presupposes that each agent only observes its own state, and not the joint state or empirical distribution of the population.

Definition 2.2 (N -player discounted regularised reward). With policies $\boldsymbol{\pi} := (\pi^1, \dots, \pi^N) \in \Pi^N$ and initial states sampled from an initial distribution $v_0 \in \Delta_{\mathcal{S}}$, the expected discounted regularised returns of each agent i in the symmetric anonymous game are given by

$$J_h^i(\boldsymbol{\pi}, v_0) = \mathbb{E} \left[\sum_{t=0}^{\infty} \gamma^t (R(s_t^i, a_t^i, \hat{\mu}_t) + h(\pi^i(s_t^i))) \middle| \begin{array}{l} s_0^j \sim v_0 \\ a_t^j \sim \pi^j(s_t^j) \\ s_{t+1}^j \sim P(\cdot | s_t^j, a_t^j, \hat{\mu}_t) \end{array}, \forall t \geq 0, j \in \{1, \dots, N\} \right],$$

where $\gamma \in [0,1)$ is a discount factor. □

Definition 2.3 (δ -Nash equilibrium). For $\delta > 0$, an initial distribution $v_0 \in \Delta_{\mathcal{S}}$ and an N -tuple of policies $\boldsymbol{\pi} := (\pi^1, \dots, \pi^N) \in \Pi^N$ form an δ -Nash equilibrium $(\boldsymbol{\pi}, v_0)$ if $\forall i = 1, \dots, N$

$$J_h^i(\boldsymbol{\pi}, v_0) \geq \max_{\pi \in \Pi} J_h^i((\pi, \boldsymbol{\pi}^{-i}), v_0) - \delta,$$

where $(\pi, \boldsymbol{\pi}^{-i}) := (\pi^1, \dots, \pi^{i-1}, \pi, \pi^{i+1}, \dots, \pi^N) \in \Pi^N$. □

At the limit as $N \rightarrow \infty$, the population of infinitely many (infinitesimal) agents, against which the representative agent plays, can be characterised as a limit distribution $\mu \in \Delta_{\mathcal{S}}$. We denote the expected discounted reward of the representative agent in the infinite-agent game - termed an MFG - as V , rather than J as in the finite N -agent case.

Definition 2.4 (Mean-field discounted regularised reward). Given a policy-population pair $(\pi, \mu) \in \Pi \times \Delta_{\mathcal{S}}$,

$$V_h(\pi, \mu) = \mathbb{E} \left[\sum_{t=0}^{\infty} \gamma^t (R(s_t, a_t, \mu) + h(\pi(s_t))) \middle| \begin{array}{l} s_0 \sim \mu \\ a_t \sim \pi(s_t) \\ s_{t+1} \sim P(\cdot | s_t, a_t, \mu) \end{array} \right]. \quad \square$$

A stationary MFG is one that has a unique population distribution that is stable with respect to a given policy, and the agents' policies are not time-dependent.

Definition 2.5 (Nash equilibrium of stationary MFG). For a policy $\pi^* \in \Pi$ and a population distribution $\mu^* \in \Delta_{\mathcal{S}}$, the pair (π^*, μ^*) is a stationary MFE if the following optimality and stability conditions hold:

$$\text{optimality: } V_h(\pi^*, \mu^*) = \max_{\pi} V_h(\pi, \mu^*),$$

$$\text{stability: } \mu^*(s) = \sum_{s', a'} \mu^*(s') \pi^*(a' | s') P(s | s', a', \mu^*).$$

If the optimality condition is only satisfied with $V_h(\pi_\delta^*, \mu_\delta^*) \geq \max_\pi V_h(\pi, \mu_\delta^*) - \delta$, then $(\pi_\delta^*, \mu_\delta^*)$ is a δ -Nash equilibrium of the MFG. \square

Crucially, the MFG Nash equilibrium is an approximate Nash equilibrium of the N -player game, which is very difficult to solve in itself.

Proposition 2.1 (N -player Nash equilibrium and MFG Nash equilibrium (Theorem 4.1, [44])). If (π^*, μ^*) is a MFG Nash equilibrium, then, under the continuity assumptions given in [44], for any $\delta > 0$, there exists $N(\delta) \in \mathbb{N}_{>0}$ such that, for all $N \geq N(\delta)$, the joint policy $\pi = \{\pi^*, \pi^*, \dots, \pi^*\} \in \Pi^N$ is a δ -Nash equilibrium of the N -player symmetric anonymous game. \square

Remark 2.1. Our theoretical analysis inherits the continuity assumptions from Yardim et al. [43] and by extension those in Saldi et al. [44]. These assumptions, which most notably include functions continuity, are not the focus of our work, so we do not detail them fully here. \square

Remark 2.2. It can be additionally shown that (π^*, μ^*) is an $\mathcal{O}(\frac{1}{\sqrt{N}})$ -Nash equilibrium of the N -player symmetric anonymous game [43, Theorem 1]. \square

For our new, networked learning algorithm, we also introduce the concept of a time-varying communication network, where the links between agents that make up the network may change at each time step t . Most commonly we might think of such a network as depending on the spacial locations of decentralised agents, such as physical robots, which can communicate with neighbours that fall within a given broadcast radius. When the agents move in the environment, their neighbours and therefore communication links will change. However, the varying network can also depend on other factors that may or may not depend on each agent's state s_t^i . For example, even a network of fixed-location agents can change depending on which agents are active broadcasting at a given time t , or if their broadcast radius changes, perhaps in relation to signal or battery strength.

Definition 2.6 (Time-varying communication network). The time-varying communication network $\{\mathcal{G}_t\}_{t \geq 0}$ is given by $\mathcal{G}_t = (\mathcal{N}, \mathcal{E}_t)$, where \mathcal{N} is the set of vertices each representing an agent $i \in \{1, \dots, N\}$, and the edge set $\mathcal{E}_t \subseteq \{(i, j) : i, j \in \mathcal{N}, i \neq j\}$ is the set of undirected communication links by which information can be shared at time t . \square

We say that a network is *connected* if there is a sequence of distinct edges that form a path between each distinct pair of vertices. The *union* of a collection of graphs $\{\mathcal{G}_t, \mathcal{G}_{t+1}, \dots, \mathcal{G}_{t+\tau}\}$ is the graph with vertices and edge set equalling the union of the vertices and edge sets of the graphs in the collection [83]. We say that the collection is *jointly connected* if the union of its members is a connected network. When considering changes in population size, for simplicity of notation we presume these occur outside of communication rounds, but this is not required by our algorithm. If agents are both leaving and (re)joining the population, we assume vertices/agents are indexed uniquely, rather than strictly from $1, \dots, N$.

3 Learning with networked, decentralised agents

3.1 Learning with N agents from a single evolution of the system

We begin by outlining the basic procedure for solving the MFG using the N agent empirical distribution and a single evolution of the system. The two underlying operators are the same for the centralised, independent and networked architectures; in the latter two cases all agents apply the operators individually, while in the centralised setting a single central agent estimates the value function and computes an updated policy that is pushed to all the other agents.

We first define, for $h_{max} > 0$ and $h : \Delta_{\mathcal{A}} \rightarrow [0, h_{max}]$, $u_{max} \in \Delta_{\mathcal{A}}$ such that $h(u_{max}) = h_{max}$. We further define $q_{max} := \frac{1+h_{max}}{1-\gamma}$, and set $\pi_{max} \in \Pi$ such that $\pi_{max}(s) = u_{max}, \forall s \in \mathcal{S}$. For any $\Delta h \in \mathbb{R}_{>0}$, we also define the convex set $\mathcal{U}_{\Delta h} := \{u \in \Delta_{\mathcal{A}} : h(u) \geq h_{max} - \Delta h\}$.

Learning agents use the stochastic TD-learning operator to estimate the Q-function of their current policy with respect to the current empirical distribution:

Definition 3.1 (Stochastic TD-learning operator, updated from (Definition 10, Yardim et al. [43])). We define $\mathcal{Z} := \mathcal{S} \times \mathcal{A} \times [0, 1] \times \mathcal{S} \times \mathcal{A}$, and say that ζ_t^i is the transition observed by agent i at time t , given by $\zeta_t^i = (s_t^i, a_t^i, r_t^i, s_{t+1}^i, a_{t+1}^i)$. The TD-learning operator $\tilde{F} : \mathcal{Q} \times \mathcal{Z} \times \beta \rightarrow \mathcal{Q}$ is defined,

for any $Q \in \mathcal{Q}, \zeta_t \in \mathcal{Z}, \beta \in \mathbb{R}$, as

$$\tilde{F}^\pi(Q, \zeta_t, \beta) = Q(s_t, a_t) - \beta (Q(s_t, a_t) - r_t - h(\pi(s_t)) - \gamma(Q(s_{t+1}, a_{t+1}))). \quad \square$$

Having estimated the Q-function of their current policy, agents improve this policy by selecting, for each state, a probability distribution over their actions that maximises the combination of three terms (Definition 3.2): 1. the value of the given state with respect to the estimated value function; 2. a regulariser over the action probability distribution (in practice, we seek to maximise the scaled entropy of the distribution); 3. a metric of similarity between the new action probabilities for the given state and those of the previous policy, given by the squared two-norm on the difference between the two distributions. We can alter the importance of the similarity metric relative to the other two terms by varying a parameter η , which is equivalent to changing the learning rate of the policy update. The three terms in the maximisation function can be seen in the policy mirror ascent (PMA) operator:

Definition 3.2 (Policy mirror ascent operator (Definition 9, Yardim et al. [43])). For a learning rate $\eta > 0$, the policy mirror ascent update operator $\Gamma_\eta^{md} : \mathcal{Q} \times \Pi \rightarrow \Pi$ is defined as

$$\Gamma_\eta^{md}(Q, \pi)(s) = \arg \max_{u \in \mathcal{U}_{L_h}} \langle u, q(s, \cdot) \rangle + h(u) - \frac{1}{2\eta} \|u - \pi(s)\|_2^2, \quad \forall s \in \mathcal{S}, \forall Q \in \mathcal{Q}, \forall \pi \in \Pi. \quad \square$$

Remark 3.1. The constant L_h , defined in Lemma 3 of Yardim et al. [43], is required theoretically for Lipschitz continuity. While our empirical results may rely on the bounds for \mathcal{U}_{L_h} , we did not find our results to be sensitive to our selection of L_h , so we do not elaborate on its structure further. \square

The learning algorithm has three nested loops. The policy update is applied K times. Before the policy update in each k loop, agents update their estimate of the Q-function by applying the stochastic TD-learning operator M_{pg} times. Prior to the TD update in each of the M_{pg} loops, agents take M_{td} steps in the environment without updating. The M_{td} loops exist to create a delay between each TD update to reduce bias when using the empirical distribution to approximate the mean field [84].

3.2 Decentralised communication scheme between networked agents

Our communication-based mean-field learning architecture combines the advantages of the centralised and independent settings. Agents compute policy updates in a decentralised manner (as in the independent case), before broadcasting their updated policy to their neighbours. Agents are equipped with a mechanism for deciding which received policy to adopt, such that the population approaches consensus as information is spread through the network. This new method brings multiple benefits when learning with an N -agent empirical distribution via a single continued evolution of the system. Firstly, communicating policies through the population means that the population as a whole is the repository of learnt information rather than specific individuals or a centralised controller. This gives the system flexibility and redundancy when faced with failure by learners or other unanticipated population changes, which outperform the other architectures; for further discussion see Appendix B.

Moreover, even in the absence of such scenarios, seeking policy consensus through communication means that the networked architecture can outperform the sample guarantees of the independent setting. For an arbitrary policy $\bar{\pi} \in \Pi$, the population's policy divergence is defined as $\Delta_{\bar{\pi}} := \frac{1}{N} \sum_i \|\bar{\pi} - \pi^i\|_1$, where $\|\pi - \pi'\|_1 := \sup_{s \in \mathcal{S}} \|\pi(s) - \pi'(s)\|_1$ for $\pi, \pi' \in \Pi$. Recall that we are approximating the Nash equilibrium of the N -agent game with the MFE, but that the N -agent empirical distribution deviates from the mean field. In fact, when agents follow different policies to each other due to independent learning and updates, such that $\Delta_{\bar{\pi}} > 0$, additional bias is incurred in the empirical population distribution [43, Lemma 7]. In turn, this divergence adds bias to the agents' value estimation with respect to the empirical distribution (via the TD-learning operator in Definition 3.1), such that settings that have lower policy divergence will have better finite sample guarantees than ones that do not [43, Theorem 1]. This explains the worse sample guarantees of the independent algorithm than the centralised one (for which $\Delta_{\bar{\pi}} = 0$); as such, networking allows us to improve on the former without requiring the latter.

The policy communication and consensus steps of Algorithm 1 occur in Lines 11-18, after the basic learning stages described in Section 3.1 in Lines 3-10. After updating their policies individually (Line 10), agents compute a number σ_{k+1}^i associated with their new policy (Line 11), and broadcast this policy and the number to their neighbours (in a function approximation setting, they would broadcast the policy parameters with the number). Agents either keep their own updated policy or adopt one

Algorithm 1 Networked learning during a single system evolution

Require: loop parameters K, M_{pg}, M_{td}, C , learning parameters $\eta, \{\beta_m\}_{m \in \{0, \dots, M_{pg}-1\}}, \lambda, \gamma$

Require: initial states $\{s_0^i\}_i, i = 1, \dots, N$

- 1: Set $\pi_0^i = \pi_{max}, \forall i$ and $t \leftarrow 0$
- 2: **for** $k = 0, \dots, K - 1$ **do**
- 3: $\forall s, a, i : \hat{Q}_0^i(s, a) = Q_{max}$
- 4: **for** $m = 0, \dots, M_{pg} - 1$ **do**
- 5: **for** M_{td} iterations **do**
- 6: Take step $\forall i : a_t^i \sim \pi_k^i(\cdot | s_t^i), r_t^i = R(s_t^i, a_t^i, \hat{\mu}_t), s_{t+1}^i \sim P(\cdot | s_t^i, a_t^i, \hat{\mu}_t); t \leftarrow t + 1$
- 7: **end for**
- 8: Compute TD update ($\forall i$): $\hat{Q}_{m+1}^i = \tilde{F}^{\pi_k^i}(\hat{Q}_m^i, \zeta_{t-2}^i, \beta_m)$ (see Definition 3.1)
- 9: **end for**
- 10: PMA step $\forall i : \pi_{k+1}^i = \Gamma_\eta^{md}(\hat{Q}_{M_{pg}}^i, \pi_k^i)$ (see Definition 3.2)
- 11: $\forall i : \sigma_{k+1}^i = \|\pi_{k+1}^i - \pi_k^i\|_1$
- 12: **for** C rounds **do**
- 13: $\forall i : \text{Broadcast } \sigma_{k+1}^i, \pi_{k+1}^i$
- 14: $\forall i : J_t^i = \{j \in \mathcal{N} : (i, j) \in \mathcal{E}_t\}$
- 15: $\forall i : \text{chosen}^i = \arg \min_{x \in \{i \cup J_t^i\}} \sigma_{k+1}^x$
- 16: $\forall i : \sigma_{k+1}^i = \sigma_{k+1}^{\text{chosen}^i}, \pi_{k+1}^i = \pi_{k+1}^{\text{chosen}^i}$
- 17: Take step $\forall i : a_t^i \sim \pi_{k+1}^i(\cdot | s_t^i), r_t^i = R(s_t^i, a_t^i, \hat{\mu}_t), s_{t+1}^i \sim P(\cdot | s_t^i, a_t^i, \hat{\mu}_t); t \leftarrow t + 1$
- 18: **end for**
- 19: **end for**
- 20: Return policies $\{\pi_K^i\}_i, i = 1, \dots, N$

of the updated policies received from their neighbours, selecting the one with the lowest associated number (Line (15)). They then take a step in the environment (Line 17), and the process may repeat for a number of rounds dictated by the parameter C .

3.3 Properties of policy adoption via communication over the network

Theorem 3.1. For any $i, j \in \{1, \dots, N\}$, the adoption of π_{k+1}^i by agent j reduces $\Delta_{\bar{\pi}}$. (Proof in Appendix D.1) \square

The more agents that adopt others' policies, the smaller the policy divergence; policy adoption can lead to complete population consensus in a number of scenarios. If the network \mathcal{G}_t representing the communication links between agents remains static and connected, then a consensus on the minimum value of σ_{k+1}^i (and hence on a single policy for the whole population) should be achieved within a number of rounds C equal to the diameter of the network [85], regardless of the method for generating σ_{k+1}^i . Since we cannot guarantee that the graph is connected when the communication rounds begin, nor that we would know the diameter of the network, we loosen these assumptions as follows. Firstly, the agents take a step in the environment during each communication round (Line 17), which may lead to a change in the communication network \mathcal{G}_t . This may especially occur in settings where the network depends on the agents' location: the agents' entropy-regularised policies means that they explore continuously, such that they may fall within communication range of each other as they move about, and the network (or the sequence $\{\mathcal{G}_t, \mathcal{G}_{t+1}, \dots, \mathcal{G}_{t+C}\}$) may become (jointly) connected. This may mean that the population comes to agree on a unique policy (giving $\Delta_{\bar{\pi}} = 0$) if C is large enough for the sequence to be jointly connected sufficiently often.

Even when the population is not left with a single common policy after C communication rounds, $\Delta_{\bar{\pi}}$ will nevertheless have been reduced due to some agents adopting the policies of others (Theorem 3.1); moreover our method for computing σ_{k+1}^i (Line 11) improves the likelihood of reducing the divergence between the remaining policies. For further discussion, see Appendix C.

Theorem 3.2. Let us say that at iteration k all agents share policy π_k , and after updating their policies they are each left with distinct π_{k+1}^i . After C communication rounds the population is left with $1 < |\Psi| < N$ policies denoted by the set Ψ . If our method for selecting which policies π_{k+1}^i to add to Ψ (i.e. which policies to keep after communication) relies on minimising $\|\pi_{k+1}^i - \pi_k\|_1$, we

also reduce an upper bound on the distance between any two members of Ψ . (Proof in Appendix D.2.) \square

3.4 Theoretical analysis and sample complexity of Algorithm 1

The sample complexity of Algorithm 1 is upper bounded by that for the independent algorithm in Yardim et al. [43]. Recall from Remark 2.2 that the MFG Nash equilibrium (π^*, μ^*) is an $\mathcal{O}(\frac{1}{\sqrt{N}})$ -Nash equilibrium of the N -player symmetric anonymous game.

Theorem 3.3. Let the independent Algorithm 3 in Yardim et al. [43] be run according to the assumptions and parameter values given in Theorem 3 of Yardim et al. [43], and our networked Algorithm 1 be run with the same parameters. In particular, note that for an arbitrary error $\epsilon > 0$, we require $K > \frac{\log 8\epsilon^{-1}}{\log L_{\Gamma_\eta}^{-1}}$, where L_{Γ_η} is a Lipschitz constant defined in Lemma 6 of Yardim et al.

[43]. Call $\pi^{i,ind}$ the policy of agent i under the independent algorithm and $\pi^{j,net}$ the policy of agent j under our networked algorithm. π^* is the unique MFG Nash equilibrium policy. Then for all agents $i = 1, \dots, N$ and $j = 1, \dots, N$, there exists a finite constant χ such that the (random) outputs $\{\pi_K^{i,ind}\}_i$ and $\{\pi_K^{j,net}\}_j$ of the algorithms satisfy

$$\mathbb{E}[\|\pi_K^{j,net} - \pi^*\|_1] \leq \mathbb{E}[\|\pi_K^{i,ind} - \pi^*\|_1] \leq \epsilon + \frac{\chi}{\sqrt{N}}. \quad \square$$

In other words, to achieve the same error ϵ , the same or fewer iterations K are required in the networked case. (Proof in Appendix D.3.)

Corollary 3.1. As $K \rightarrow \infty$, $\epsilon \rightarrow 0$, such that the networked algorithm asymptotically converges to an $\mathcal{O}(\frac{1}{\sqrt{N}})$ -Nash equilibrium of the N -player symmetric anonymous game. \square

3.5 Algorithm acceleration by use of experience-replay buffer

Our theoretical analysis requires hyperparameters, discussed fully in Appendix E, that render the algorithm’s convergence impractically slow. In order to empirically show the benefits of our networked architecture in comparison to the centralised and independent baselines, we modify Algorithm 1 as follows, with the changes shown in *blue* in Algorithm 2 in Appendix E. We similarly modify the centralised and independent algorithms. Instead of using a transition ζ_{t-2}^i to compute the TD update within each M_{pg} iteration and then discarding the transition, we store the transition in a replay buffer (Line 11) and postpone learning until after the M_{pg} loops (Lines 14-19). Replay buffers are a common RL tool used in particular with deep learning, precisely to improve data efficiency and reduce autocorrelation [86; 87]. When learning does take place in our modified algorithm, it involves cycling through the buffer for L iterations (Line 14) - randomly shuffling the buffer between each - and hence conducting the TD update on each stored transition multiple times. This allows us to reduce the number of M_{pg} loops (and in turn the nested M_{td} loops), as well as not requiring as small a learning rate $\{\beta_m\}_{m \in \{0, \dots, M_{pg}-1\}}$ as that defined in Theorem 1 of Yardim et al. [43], allowing much faster learning in practice. We leave β fixed across all iterations, as we found empirically that this simple scheme gave sufficient learning. We have not experimented with decreasing β as $l \in L$ increases, though this may benefit learning.

Moreover, by shuffling the buffer before each cycle we reduce bias resulting from the dependency of samples along the single path, which may be a reason for us being able to achieve adequate stable learning even when reducing the number of M_{td} waiting steps within each M_{pg} loop. Due to reducing M_{td} , we add a parameter that causes agents to wait for W iterations of the M_{pg} loop before adding transitions to the buffer (Line 10), to ensure the population settles to the new empirical distribution after a policy update, before learning resumes. Shuffling may also help to loosen the ergodicity assumption necessary for the sample guarantees given in Yardim et al. [43], which would not hold for some policies in certain settings which lead to periodicity in the Markov chain [42].

4 Experiments

We follow prior works on stationary MFGs in the types of game chosen for our demonstrations [19; 42; 55; 67; 88]. We focus on grid-world environments in which agents’ actions consist of moving

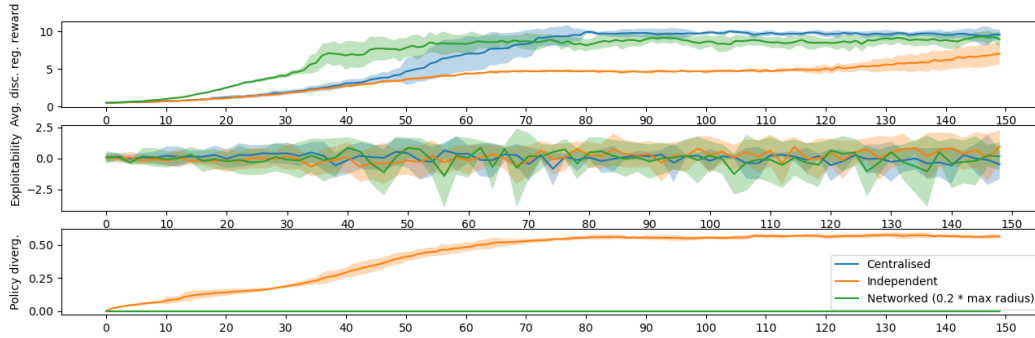


Figure 1: Agree on a single target - 50% chance of learning failure at every iteration.

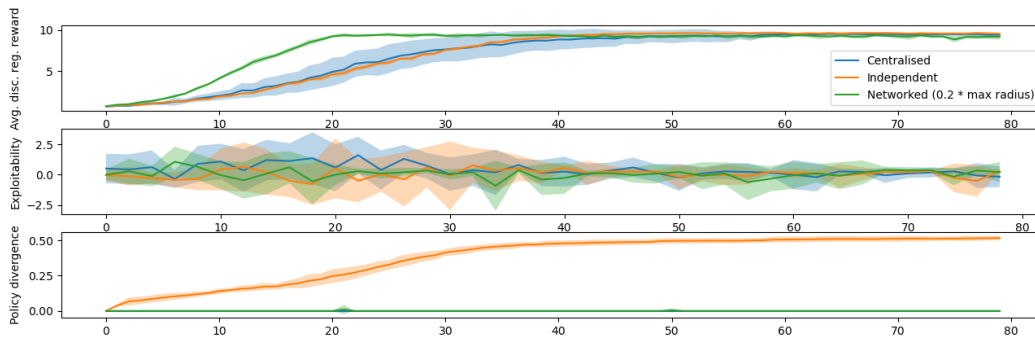


Figure 2: Diffuse across multiple targets - 50% chance of learning failure at every iteration.

in one of the four cardinal directions or remaining in place. We present results from two tasks defined by the reward functions of the agents; see Appendix F.1 for an extended technical description of our task settings, as well as experiments on a third game. In experiments involving target locations, we place one in each of the four corners of the grid.

Agree on a single target. The agents are rewarded for visiting any target, but their reward is proportional to the number of other agents collocated at that target. The agents must therefore agree on which one target they will all visit to maximise their individual rewards.

Diffuse across multiple targets. Similar to the ‘crowd modelling with congestion’ game in [19; 67], the agents are rewarded for visiting any target, but must avoid unbalanced aggregation at the targets, such that the targets should receive equal coverage from the population.

For each task, we conduct tests in two settings, reflecting the scenarios elaborated in Appendix B. The first illustrates robustness to learning failures: the population has 200 agents throughout, but at every iteration k each learner fails to update its policy with a 50% probability. The second test illustrates scalability and robustness to increases in population size. The population begins with 25 agents learning normally, and a further 175 agents are added to the population at a certain point in the run. Hyperparameters are discussed in Appendix F.4.

4.1 Evaluation metrics

Works on MFGs often use the *exploitability* metric to evaluate how close a given policy π is to the MFE policy π^* [19; 20; 45; 67; 89]. However, this metric has previously been used in centralised settings where the whole population shares a single policy, and it becomes problematic when agents may follow different policies, as in the independent and, possibly, the networked case. For a full discussion, see Appendix F.2. In lieu of a single satisfactory metric, we instead present several proxies to give as informative results as possible about both performance and proximity to the Nash equilibrium. These are: Approximation of the **exploitability of the joint policy π** - this is the

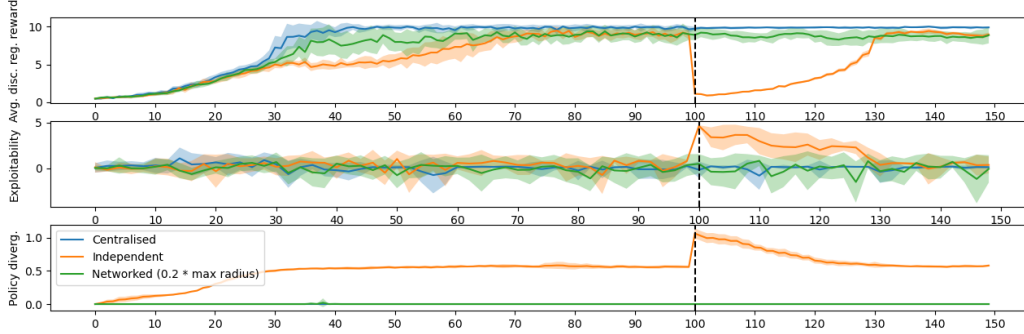


Figure 3: Agree on a single target - an extra 175 agents enter the population at iteration 100.

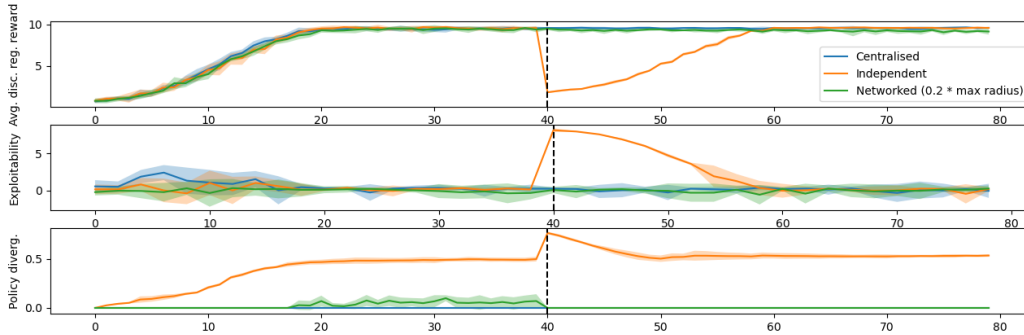


Figure 4: Diffuse across multiple targets - an extra 175 agents enter the population at iteration 40.

standard exploitability metric in the centralised case, and frequently also in the networked case, whenever agents reach policy consensus within the C communication rounds. Due to the expensive computations required for this metric, we evaluate it on alternate k iterations. **Average discounted regularised reward of the agents’ policies** π^i - since our approximation of the exploitability metric is often noisy, in some settings it can be difficult to discern from this how our networked algorithm compares to the baselines. The discounted return gives a clearer sense of how well the population is performing, though with the same caveat as the previous metric that in the independent case, this return reflects the achievement of the *joint* policy, rather than the suitability of any one policy (see Appendix F.3). Given the issues with these metrics in the independent case (and to a much lesser extent, in the networked case), we also include: the **population’s policy divergence** $\Delta_{\pi^1} := \frac{1}{N} \sum_i \|\pi^1 - \pi^i\|_1$, where $\|\pi - \pi'\|_1 := \sup_{s \in \mathcal{S}} \|\pi(s) - \pi'(s)\|_1$. If the policies are diverging, as often seen in the independent case (and to a much lesser extent, in the networked case), this suggests that they are not approaching the equilibrium policy π^* , even if the exploitability and return of the joint policy are performing similarly to the centralised and networked cases.

4.2 Discussion

Our plots show that the centralised architecture is always ultimately able to achieve the highest average return, but we can see that, aside from raising strong assumptions, it suffers from the disadvantage of presenting a single point of failure, such that the networked architecture learns faster in the face of a 50% failure rate. Our networked algorithm likewise demonstrates greater robustness than the independent algorithm both to agent failures and population increases, as can be seen by the latter’s slower learning in Plots 1 and 2, and large drop in return and increase in exploitability in Plots 3 and 4. Moreover, as predicted in Section 3.4, Plot 3 shows our networked algorithm increasing its return faster than independent case, even when no learning failures occur.

We emphasise again that the large and increasing policy divergence of the independent learners in every experiment highlights that the return and exploitability of the joint policy are misleading

metrics for this algorithm when viewed alone, as the population is able to perform superficially well without approaching a single MFE policy. The ‘diffuse across multiple targets’ task is particularly conducive to such ‘cheating’, since it is easier to move to different corners of the grid when policies differ. However, this unintended solution may not be desired in all settings (see Appendix F.3).

For limitations and ongoing work, see Appendix G, and find additional experiments in Appendix F.5.

Acknowledgments and Disclosure of Funding

We would like to thank Sriram Ganapathi Subramanian for helpful discussions in the initial stages of this project. Patrick Benjamin is supported by the UK EPSRC Centre for Doctoral Training in Autonomous Intelligent Machines and Systems with the grant EP/S024050/1.

References

- [1] Lucian Busoniu, Robert Babuska, and Bart De Schutter. A Comprehensive Survey of Multi-agent Reinforcement Learning. *IEEE Transactions on Systems, Man, and Cybernetics, Part C (Applications and Reviews)*, 38(2):156–172, 2008. doi: 10.1109/TSMCC.2007.913919.
- [2] Kaiqing Zhang, Zhuoran Yang, and Tamer Başar. *Multi-Agent Reinforcement Learning: A Selective Overview of Theories and Algorithms*, pages 321–384. Springer International Publishing, Cham, 2021. ISBN 978-3-030-60990-0. doi: 10.1007/978-3-030-60990-0_12. URL https://doi.org/10.1007/978-3-030-60990-0_12.
- [3] Richard S Sutton and Andrew G Barto. *Reinforcement Learning: An Introduction*. MIT press, 2018.
- [4] David L. Leottau, Javier Ruiz del Solar, and Robert Babuka. Decentralized Reinforcement Learning of Robot Behaviors. *Artificial Intelligence*, 256:130–159, 2018. ISSN 0004-3702. doi: <https://doi.org/10.1016/j.artint.2017.12.001>. URL <https://www.sciencedirect.com/science/article/pii/S0004370217301674>.
- [5] Zefang Lv, Liang Xiao, Yousong Du, Guohang Niu, Chengwen Xing, and Wenyuan Xu. Multi-Agent Reinforcement Learning based UAV Swarm Communications Against Jamming. *IEEE Transactions on Wireless Communications*, pages 1–1, 2023. doi: 10.1109/TWC.2023.3268082.
- [6] James Orr and Ayan Dutta. Multi-Agent Deep Reinforcement Learning for Multi-Robot Applications: A Survey. *Sensors*, 23(7), 2023. ISSN 1424-8220. doi: 10.3390/s23073625. URL <https://www.mdpi.com/1424-8220/23/7/3625>.
- [7] Shai Shalev-Shwartz, Shaked Shammah, and Amnon Shashua. Safe, multi-agent, reinforcement learning for autonomous driving. *arXiv preprint arXiv:1610.03295*, 2016.
- [8] Patrick Mannion, Jim Duggan, and Enda Howley. *An Experimental Review of Reinforcement Learning Algorithms for Adaptive Traffic Signal Control*, pages 47–66. Springer International Publishing, Cham, 2016. ISBN 978-3-319-25808-9. doi: 10.1007/978-3-319-25808-9_4. URL https://doi.org/10.1007/978-3-319-25808-9_4.
- [9] Mikayel Samvelyan, Tabish Rashid, Christian Schroeder de Witt, Gregory Farquhar, Nantas Nardelli, Tim G. J. Rudner, Chia-Man Hung, Philip H. S. Torr, Jakob Foerster, and Shimon Whiteson. The StarCraft Multi-Agent Challenge. In *Proceedings of the 18th International Conference on Autonomous Agents and MultiAgent Systems*, AAMAS ’19, page 2186–2188, Richland, SC, 2019. International Foundation for Autonomous Agents and Multiagent Systems. ISBN 9781450363099.
- [10] Oriol Vinyals, Igor Babuschkin, Junyoung Chung, Michael Mathieu, Max Jaderberg, Wojtek Czarnecki, Andrew Dudzik, Aja Huang, Petko Georgiev, Richard Powell, Timo Ewalds, Dan Horgan, Manuel Kroiss, Ivo Danihelka, John Agapiou, Junhyuk Oh, Valentin Dalibard, David Choi, Laurent Sifre, Yury Sulsky, Sasha Vezhnevets, James Molloy, Trevor Cai, David Budden, Tom Paine, Caglar Gulcehre, Ziyu Wang, Tobias Pfaff, Toby Pohlen, Dani Yogatama, Julia Cohen, Katrina McKinney, Oliver Smith, Tom Schaul, Timothy Lillicrap, Chris Apps, Koray Kavukcuoglu, Demis Hassabis, and David Silver. AlphaStar: Mastering the Real-Time Strategy Game StarCraft II. <https://deepmind.com/blog/alphastar-mastering-real-time-strategy-game-starcraft-ii/>, 2019.
- [11] OpenAI, Christopher Berner, Greg Brockman, Brooke Chan, Vicki Cheung, Przemysław Dębiak, Christy Dennison, David Farhi, Quirin Fischer, Shariq Hashme, Chris Hesse, Rafal Józefowicz, Scott Gray, Catherine Olsson, Jakub Pachocki, Michael Petrov, Henrique P. d. O. Pinto, Jonathan Raiman, Tim Salimans, Jeremy Schlatter, Jonas Schneider, Szymon Sidor, Ilya Sutskever, Jie Tang, Filip Wolski, and Susan Zhang. Dota 2 with Large Scale Deep Reinforcement Learning, 2019.
- [12] Joel Z. Leibo, Vinicius Zambaldi, Marc Lanctot, Janusz Marecki, and Thore Graepel. Multi-Agent Reinforcement Learning in Sequential Social Dilemmas. In *Proceedings of the 16th Conference on Autonomous Agents and MultiAgent Systems*, AAMAS ’17, page 464–473, Richland, SC, 2017. International Foundation for Autonomous Agents and Multiagent Systems.

- [13] Kris Cao, Angeliki Lazaridou, Marc Lanctot, Joel Z. Leibo, Karl Tuyls, and Stephen Clark. Emergent Communication through Negotiation. In *International Conference on Learning Representations*, 2018. URL <https://openreview.net/forum?id=Hk6WhagRW>.
- [14] Natasha Jaques, Angeliki Lazaridou, Edward Hughes, Caglar Gulcehre, Pedro A. Ortega, DJ Strouse, Joel Z. Leibo, and Nando de Freitas. Social Influence as Intrinsic Motivation for Multi-Agent Deep Reinforcement Learning, 2019.
- [15] Kevin R. McKee, Ian Gemp, Brian McWilliams, Edgar A. Duéñez-Guzmán, Edward Hughes, and Joel Z. Leibo. Social diversity and social preferences in mixed-motive reinforcement learning, 2020.
- [16] Navid Rashedi. Markov game approach for multi-agent competitive bidding strategies in electricity market. *IET Generation, Transmission & Distribution*, 10:3756–3763(7), November 2016. ISSN 1751-8687. URL <https://digital-library.theiet.org/content/journals/10.1049/iet-gtd.2016.0075>.
- [17] Ali Shavandi and Majid Khedmati. A multi-agent deep reinforcement learning framework for algorithmic trading in financial markets. *Expert Systems with Applications*, 208:118124, 2022. ISSN 0957-4174. doi: <https://doi.org/10.1016/j.eswa.2022.118124>. URL <https://www.sciencedirect.com/science/article/pii/S0957417422013082>.
- [18] Constantinos Daskalakis, Paul W. Goldberg, and Christos H. Papadimitriou. The Complexity of Computing a Nash Equilibrium. In *Proceedings of the Thirty-Eighth Annual ACM Symposium on Theory of Computing*, STOC '06, page 71–78, New York, NY, USA, 2006. Association for Computing Machinery. ISBN 1595931341. doi: 10.1145/1132516.1132527. URL <https://doi.org/10.1145/1132516.1132527>.
- [19] Mathieu Laurière, Sarah Perrin, Sertan Girgin, Paul Muller, Ayush Jain, Theophile Cabbannes, Georgios Piliouras, Julien Pérolat, Romuald Élie, Olivier Pietquin, and Matthieu Geist. Scalable Deep Reinforcement Learning Algorithms for Mean Field Games, 2022. URL <https://arxiv.org/abs/2203.11973>.
- [20] Sarah Perrin, Julien Pérolat, Mathieu Laurière, Matthieu Geist, Romuald Elie, and Olivier Pietquin. Fictitious Play for Mean Field Games: Continuous Time Analysis and Applications. In *Proceedings of the 34th International Conference on Neural Information Processing Systems*, NIPS'20, Red Hook, NY, USA, 2020. Curran Associates Inc. ISBN 9781713829546.
- [21] Qiaomin Xie, Zhuoran Yang, Zhaoran Wang, and Andreea Minca. Learning While Playing in Mean-Field Games: Convergence and Optimality. In Marina Meila and Tong Zhang, editors, *Proceedings of the 38th International Conference on Machine Learning*, volume 139 of *Proceedings of Machine Learning Research*, pages 11436–11447. PMLR, 18–24 Jul 2021. URL <https://proceedings.mlr.press/v139/xie21g.html>.
- [22] Oriol Vinyals, Igor Babuschkin, Wojciech M. Czarnecki, Michaël Mathieu, Andrew Dudzik, Junyoung Chung, David H. Choi, Richard Powell, Timo Ewalds, Petko Georgiev, Junhyuk Oh, Dan Horgan, Manuel Kroiss, Ivo Danihelka, Aja Huang, L. Sifre, Trevor Cai, John P. Agapiou, Max Jaderberg, Alexander Sasha Vezhnevets, Rémi Leblond, Tobias Pohlen, Valentin Dalibard, David Budden, Yury Sulsky, James Molloy, Tom Le Paine, Caglar Gulcehre, Ziyun Wang, Tobias Pfaff, Yuhuai Wu, Roman Ring, Dani Yogatama, Dario Wünsch, Katrina McKinney, Oliver Smith, Tom Schaul, Timothy P. Lillicrap, Koray Kavukcuoglu, Demis Hassabis, Chris Apps, and David Silver. Grandmaster level in StarCraft II using multi-agent reinforcement learning. *Nature*, pages 1–5, 2019.
- [23] Stephen McAleer, JB Lanier, Roy Fox, and Pierre Baldi. Pipeline PSRO: A Scalable Approach for Finding Approximate Nash Equilibria in Large Games. In H. Larochelle, M. Ranzato, R. Hadsell, M.F. Balcan, and H. Lin, editors, *Advances in Neural Information Processing Systems*, volume 33, pages 20238–20248. Curran Associates, Inc., 2020. URL https://proceedings.neurips.cc/paper_files/paper/2020/file/e9bcd1b063077573285ae1a41025f5dc-Paper.pdf.

- [24] Lingxiao Wang, Zhuoran Yang, and Zhaoran Wang. Breaking the Curse of Many Agents: Provable Mean Embedding Q-Iteration for Mean-Field Reinforcement Learning. In *Proceedings of the 37th International Conference on Machine Learning, ICML'20*. JMLR.org, 2020.
- [25] Lianmin Zheng, Jiacheng Yang, Han Cai, Ming Zhou, Weinan Zhang, Jun Wang, and Yong Yu. MAgent: A Many-Agent Reinforcement Learning Platform for Artificial Collective Intelligence. In *Proceedings of the AAAI conference on artificial intelligence*, volume 32, 2018.
- [26] Kai Cui, Anam Tahir, Gizem Ekinici, Ahmed Elshamhory, Yannick Eich, Mengguang Li, and Heinz Koeppl. A Survey on Large-Population Systems and Scalable Multi-Agent Reinforcement Learning. *arXiv preprint arXiv:2209.03859*, 2022.
- [27] Daniel Jarne Ornia, Pedro J. Zufiria, and Manuel Mazo Jr. Mean Field Behavior of Collaborative Multiagent Foragers. *IEEE Transactions on Robotics*, 38(4):2151–2165, 2022. doi: 10.1109/TRO.2022.3152691.
- [28] Hamid Shiri, Jihong Park, and Mehdi Bennis. Massive Autonomous UAV Path Planning: A Neural Network Based Mean-Field Game Theoretic Approach, 2019.
- [29] Lu Chang, Liang Shan, Weilong Zhang, and Yuewei Dai. Hierarchical multi-robot navigation and formation in unknown environments via deep reinforcement learning and distributed optimization. *Robotics and Computer-Integrated Manufacturing*, 83:102570, 2023. ISSN 0736-5845. doi: <https://doi.org/10.1016/j.rcim.2023.102570>. URL <https://www.sciencedirect.com/science/article/pii/S0736584523000467>.
- [30] Torsten Trimborn, Martin Frank, and Stephan Martin. Mean field limit of a behavioral financial market model. *Physica A: Statistical Mechanics and its Applications*, 505:613–631, 2018. ISSN 0378-4371. doi: <https://doi.org/10.1016/j.physa.2018.03.079>. URL <https://www.sciencedirect.com/science/article/pii/S0378437118303984>.
- [31] Zongxi Li, A. Max Reppen, and Ronnie Sircar. A Mean Field Games Model for Cryptocurrency Mining, 2022.
- [32] Emily Meigs, Francesca Parise, Asuman E. Ozdaglar, and Daron Acemoglu. Optimal dynamic information provision in traffic routing. *CoRR*, abs/2001.03232, 2020. URL <https://arxiv.org/abs/2001.03232>.
- [33] Kuang Huang, Xuan Di, Qiang Du, and Xi Chen. A game-theoretic framework for autonomous vehicles velocity control: Bridging microscopic differential games and macroscopic mean field games. *Discrete and Continuous Dynamical Systems - B*, 25(12):4869–4903, 2020. ISSN 1531-3492. doi: 10.3934/dcdsb.2020131.
- [34] Tianfeng Hu, Zhiqun hu, Zhaoming Lu, and Xiangming Wen. Dynamic traffic signal control using mean field multi-agent reinforcement learning in large scale road-networks. *IET Intelligent Transport Systems*, pages n/a–n/a, 04 2023. doi: 10.1049/itr2.12364.
- [35] Weichao Mao, Haoran Qiu, Chen Wang, Hubertus Franke, Zbigniew T. Kalbarczyk, Ravishankar K. Iyer, and Tamer Başar. A mean-field game approach to cloud resource management with function approximation. In *Proceedings of the 36th Conference on Advances in Neural Information Processing Systems (NIPS 2022)*, volume 36, pages 1–12, New Orleans, LA, USA, 2022. Curran Associates, Inc.
- [36] Dario Bauso and Hamidou Tembine. Crowd-Averse Cyber-Physical Systems: The Paradigm of Robust Mean-Field Games. *IEEE Transactions on Automatic Control*, 61(8):2312–2317, 2016. doi: 10.1109/TAC.2015.2492038.
- [37] Rajesh Mishra, Sriram Vishwanath, and Deepanshu Vasal. Model-free Reinforcement Learning for Mean Field Games. *IEEE Transactions on Control of Network Systems*, pages 1–11, 2023. doi: 10.1109/TCNS.2023.3264934.
- [38] Jean-Michel Lasry and Pierre-Louis Lions. Mean Field Games. *Japanese Journal of Mathematics*, 2(1):229–260, 2007.

- [39] Minyi Huang, Roland P. Malhamé, and Peter E. Caines. Large population stochastic dynamic games: closed-loop McKean-Vlasov systems and the Nash certainty equivalence principle. *Communications in Information & Systems*, 6(3):221 – 252, 2006.
- [40] Rico Berner, Thilo Gross, Christian Kuehn, Jürgen Kurths, and Serhiy Yanchuk. *Adaptive Dynamical Networks*, 2023.
- [41] Berkay Anahtarci, Can Deha Karıksız, and Naci Saldi. Q-Learning in Regularized Mean-field Games. *Dynamic Games and Applications*, 13:89 – 117, 2020.
- [42] Muhammad Aneeq uz Zaman, Alec Koppel, Sujay Bhatt, and Tamer Başar. Oracle-free Reinforcement Learning in Mean-Field Games along a Single Sample Path, 2023.
- [43] Batuhan Yardim, Semih Cayci, Matthieu Geist, and Niao He. Policy Mirror Ascent for Efficient and Independent Learning in Mean Field Games, 2022. URL <https://arxiv.org/abs/2212.14449>.
- [44] Naci Saldi, Tamer Başar, and Maxim Raginsky. Markov–Nash Equilibria in Mean-Field Games with Discounted Cost. *SIAM Journal on Control and Optimization*, 56(6):4256–4287, 2018. doi: 10.1137/17M1112583. URL <https://doi.org/10.1137/17M1112583>.
- [45] Mathieu Laurière, Sarah Perrin, Matthieu Geist, and Olivier Pietquin. Learning Mean Field Games: A Survey, 2022. URL <https://arxiv.org/abs/2205.12944>.
- [46] Yves Achdou and Italo Capuzzo-Dolcetta. Mean Field Games: Numerical Methods. *SIAM Journal on Numerical Analysis*, 48(3):1136–1162, 2010. doi: 10.1137/090758477. URL <https://doi.org/10.1137/090758477>.
- [47] E. Carlini and F. J. Silva. A Fully Discrete Semi-Lagrangian Scheme for a First Order Mean Field Game Problem. *SIAM Journal on Numerical Analysis*, 52(1):45–67, 2014. doi: 10.1137/120902987. URL <https://doi.org/10.1137/120902987>.
- [48] Luis Briceño-Arias, Dante Kalise, and Francisco Silva. Proximal methods for stationary Mean Field Games with local couplings. *SIAM Journal on Control and Optimization*, 56:801–, 03 2018.
- [49] Yves Achdou and Mathieu Laurière. *Mean Field Games and Applications: Numerical Aspects*, 2020.
- [50] Xin Guo, Anran Hu, Renyuan Xu, and Junzi Zhang. A General Framework for Learning Mean-Field Games, 2020. URL <https://arxiv.org/abs/2003.06069>.
- [51] Xin Guo, Anran Hu, Renyuan Xu, and Junzi Zhang. Learning Mean-Field Games. In H. Wallach, H. Larochelle, A. Beygelzimer, F. d’Alché-Buc, E. Fox, and R. Garnett, editors, *Advances in Neural Information Processing Systems*, volume 32. Curran Associates, Inc., 2019. URL https://proceedings.neurips.cc/paper_files/paper/2019/file/030e65da2b1c944090548d36b244b28d-Paper.pdf.
- [52] Sarah Perrin, Mathieu Laurière, Julien Pérolat, Matthieu Geist, Romuald Élie, and Olivier Pietquin. Mean field games flock! the reinforcement learning way. In *IJCAI*, 2021.
- [53] Jayakumar Subramanian and Aditya Mahajan. Reinforcement Learning in Stationary Mean-Field Games. In *Proceedings of the 18th International Conference on Autonomous Agents and MultiAgent Systems, AAMAS ’19*, page 251–259, Richland, SC, 2019. International Foundation for Autonomous Agents and Multiagent Systems. ISBN 9781450363099.
- [54] Andrea Angiuli, Jean-Pierre Fouque, and Mathieu Laurière. Unified Reinforcement Q-Learning for Mean Field Game and Control Problems, 2021.
- [55] Mathieu Laurière. Numerical Methods for Mean Field Games and Mean Field Type Control, 2021.
- [56] Hamidou Tembine, Raul Tempone, and Pedro Vilanova. *Mean-Field Learning: a Survey*, 2012.

- [57] Cardaliaguet, Pierre and Hadikhanloo, Saeed. Learning in mean field games: The fictitious play. *ESAIM: COCV*, 23(2):569–591, 2017. doi: 10.1051/cocv/2016004. URL <https://doi.org/10.1051/cocv/2016004>.
- [58] Matthieu Geist, Julien Pérolat, Mathieu Laurière, Romuald Elie, Sarah Perrin, Olivier Bachem, Rémi Munos, and Olivier Pietquin. Concave Utility Reinforcement Learning: the Mean-Field Game Viewpoint, 2022.
- [59] J Frédéric Bonnans, Pierre Lavigne, and Laurent Pfeiffer. Generalized conditional gradient and learning in potential mean field games, 2021.
- [60] David Mguni, Joel Jennings, and Enrique Munoz de Cote. Decentralised Learning in Systems With Many, Many Strategic Agents. *Proceedings of the AAI Conference on Artificial Intelligence*, 32(1), Apr. 2018. doi: 10.1609/aaai.v32i1.11586. URL <https://ojs.aaai.org/index.php/AAAI/article/view/11586>.
- [61] Marcin Korecki, Damian Dailisan, and Dirk Helbing. How Well Do Reinforcement Learning Approaches Cope With Disruptions? The Case of Traffic Signal Control. *IEEE Access*, 11: 36504–36515, 2023. doi: 10.1109/ACCESS.2023.3266644.
- [62] Romuald Elie, Julien Pérolat, Mathieu Laurière, Matthieu Geist, and Olivier Pietquin. On the Convergence of Model Free Learning in Mean Field Games. *Proceedings of the AAI Conference on Artificial Intelligence*, 34(05):7143–7150, Apr. 2020. doi: 10.1609/aaai.v34i05.6203. URL <https://ojs.aaai.org/index.php/AAAI/article/view/6203>.
- [63] René Carmona and Mathieu Laurière. Deep Learning for Mean Field Games and Mean Field Control with Applications to Finance, 2021.
- [64] Haoyang Cao, Xin Guo, and Mathieu Laurière. Connecting GANs, MFGs, and OT, 2021.
- [65] Maximilien Germain, Joseph Mikael, and Xavier Warin. Numerical resolution of McKean-Vlasov FBSDEs using neural networks, 2022.
- [66] Jean-Pierre Fouque and Zhaoyu Zhang. Deep Learning Methods for Mean Field Control Problems With Delay. *Frontiers in Applied Mathematics and Statistics*, 6, 2020. ISSN 2297-4687. doi: 10.3389/fams.2020.00011. URL <https://www.frontiersin.org/articles/10.3389/fams.2020.00011>.
- [67] Talal Algumaei, Ruben Solozabal, Reda Alami, Hakim Hacid, Merouane Debbah, and Martin Takac. Regularization of the policy updates for stabilizing Mean Field Games, 2023.
- [68] Xin Guo, Anran Hu, Renyuan Xu, and Junzi Zhang. Learning Mean-Field Games, 2019. URL <https://arxiv.org/abs/1901.09585>.
- [69] Kaiqing Zhang, Zhuoran Yang, Han Liu, Tong Zhang, and Tamer Basar. Fully Decentralized Multi-Agent Reinforcement Learning with Networked Agents. In Jennifer Dy and Andreas Krause, editors, *Proceedings of the 35th International Conference on Machine Learning*, volume 80 of *Proceedings of Machine Learning Research*, pages 5872–5881. PMLR, 10–15 Jul 2018. URL <https://proceedings.mlr.press/v80/zhang18n.html>.
- [70] Hoi-To Wai, Zhuoran Yang, Zhaoran Wang, and Mingyi Hong. Multi-Agent Reinforcement Learning via Double Averaging Primal-Dual Optimization. In *Proceedings of the 32nd International Conference on Neural Information Processing Systems, NIPS’18*, page 9672–9683, Red Hook, NY, USA, 2018. Curran Associates Inc.
- [71] Kaiqing Zhang, Zhuoran Yang, and Tamer Başar. Decentralized Multi-Agent Reinforcement Learning with Networked Agents: Recent Advances, 2019. URL <https://arxiv.org/abs/1912.03821>.
- [72] Mingzhe Chen, Deniz Gündüz, Kaibin Huang, Walid Saad, Mehdi Bennis, Aneta Vulgarakis Feljan, and H. Vincent Poor. Distributed Learning in Wireless Networks: Recent Progress and Future Challenges, 2021. URL <https://arxiv.org/abs/2104.02151>.

- [73] Bora Yongacoglu, Gürdal Arslan, and Serdar Yüksel. Independent Learning in Mean-Field Games: Satisficing Paths and Convergence to Subjective Equilibria, 2022. URL <https://arxiv.org/abs/2209.05703>.
- [74] Bora Yongacoglu, Gürdal Arslan, and Serdar Yüksel. Independent Learning and Subjectivity in Mean-Field Games. In *2022 IEEE 61st Conference on Decision and Control (CDC)*, pages 2845–2850, 2022. doi: 10.1109/CDC51059.2022.9992399.
- [75] Dario Bauso, Hamidou Tembine, and Tamer Başar. Robust Mean Field Games with Application to Production of an Exhaustible Resource. *IFAC Proceedings Volumes*, 45(13):454–459, 2012. ISSN 1474-6670. doi: <https://doi.org/10.3182/20120620-3-DK-2025.00135>. URL <https://www.sciencedirect.com/science/article/pii/S1474667015377302>. 7th IFAC Symposium on Robust Control Design.
- [76] Kaiqing Zhang, Zhuoran Yang, and Tamer Başar. “Multi-Agent Reinforcement Learning: A Selective Overview of Theories and Algorithms”, pages 321–384. Springer International Publishing, Cham, 2021. ISBN 978-3-030-60990-0. doi: 10.1007/978-3-030-60990-0_12. URL https://doi.org/10.1007/978-3-030-60990-0_12.
- [77] Thinh T. Doan, Siva Theja Maguluri, and Justin Romberg. Finite-Time Analysis of Distributed TD(0) with Linear Function Approximation for Multi-Agent Reinforcement Learning, 2019. URL <https://arxiv.org/abs/1902.07393>.
- [78] Yixuan Lin, Kaiqing Zhang, Zhuoran Yang, Zhaoran Wang, Tamer Başar, Romeil Sandhu, and Ji Liu. A Communication-Efficient Multi-Agent Actor-Critic Algorithm for Distributed Reinforcement Learning. In *2019 IEEE 58th Conference on Decision and Control (CDC)*, pages 5562–5567, 2019. doi: 10.1109/CDC40024.2019.9029257.
- [79] Paulo Heredia, Hasan Ghadialy, and Shaoshuai Mou. Finite-Sample Analysis of Distributed Q-learning for Multi-Agent Networks. In *2020 American Control Conference (ACC)*, pages 3511–3516, 2020. doi: 10.23919/ACC45564.2020.9147428.
- [80] Soumya Kar, José M. F. Moura, and H. Vincent Poor. QD-Learning: A Collaborative Distributed Strategy for Multi-Agent Reinforcement Learning Through Consensus+Innovations. *IEEE Transactions on Signal Processing*, 61(7):1848–1862, 2013. doi: 10.1109/TSP.2013.2241057.
- [81] Wesley Suttle, Zhuoran Yang, Kaiqing Zhang, Zhaoran Wang, Tamer Basar, and Ji Liu. A Multi-Agent Off-Policy Actor-Critic Algorithm for Distributed Reinforcement Learning, 2019. URL <https://arxiv.org/abs/1903.06372>.
- [82] Kaiqing Zhang, Zhuoran Yang, and Tamer Basar. Networked Multi-Agent Reinforcement Learning in Continuous Spaces. In *2018 IEEE Conference on Decision and Control (CDC)*, pages 2771–2776, 2018. doi: 10.1109/CDC.2018.8619581.
- [83] A. Jadbabaie, Jie Lin, and A.S. Morse. Coordination of groups of mobile autonomous agents using nearest neighbor rules. *IEEE Transactions on Automatic Control*, 48(6):988–1001, 2003. doi: 10.1109/TAC.2003.812781.
- [84] Georgios Kotsalis, Guanghui Lan, and Tianjiao Li. Simple and Optimal Methods for Stochastic Variational Inequalities, II: Markovian Noise and Policy Evaluation in Reinforcement Learning. *SIAM Journal on Optimization*, 32(2):1120–1155, 2022. doi: 10.1137/20M1381691. URL <https://doi.org/10.1137/20M1381691>.
- [85] Shreevatsa Rajagopalan and Devavrat Shah. Distributed Averaging in Dynamic Networks. In *Proceedings of the ACM SIGMETRICS International Conference on Measurement and Modeling of Computer Systems*, SIGMETRICS ’10, page 369–370, New York, NY, USA, 2010. Association for Computing Machinery. ISBN 9781450300384. doi: 10.1145/1811039.1811091. URL <https://doi.org/10.1145/1811039.1811091>.
- [86] Long-Ji Lin. Self-Improving Reactive Agents Based on Reinforcement Learning, Planning and Teaching. *Mach. Learn.*, 8(3–4):293–321, may 1992. ISSN 0885-6125. doi: 10.1007/BF00992699. URL <https://doi.org/10.1007/BF00992699>.

- [87] William Fedus, Prajit Ramachandran, Rishabh Agarwal, Yoshua Bengio, Hugo Larochelle, Mark Rowland, and Will Dabney. Revisiting Fundamentals of Experience Replay. In *Proceedings of the 37th International Conference on Machine Learning, ICML'20*. JMLR.org, 2020.
- [88] Kai Cui, Christian Fabian, and Heinz Koepl. Multi-Agent Reinforcement Learning via Mean Field Control: Common Noise, Major Agents and Approximation Properties, 2023.
- [89] Julien Pérolat, Sarah Perrin, Romuald Elie, Mathieu Laurière, Georgios Piliouras, Matthieu Geist, Karl Tuyls, and Olivier Pietquin. Scaling Mean Field Games by Online Mirror Descent. In *Proceedings of the 21st International Conference on Autonomous Agents and Multiagent Systems, AAMAS '22*, page 1028–1037, Richland, SC, 2022. International Foundation for Autonomous Agents and Multiagent Systems. ISBN 9781450392136.
- [90] Kai Cui and Heinz Koepl. Approximately Solving Mean Field Games via Entropy-Regularized Deep Reinforcement Learning, 2021. URL <https://arxiv.org/abs/2102.01585>.
- [91] Rajesh K Mishra, Deepanshu Vasal, and Sriram Vishwanath. Model-free Reinforcement Learning for Non-stationary Mean Field Games. In *2020 59th IEEE Conference on Decision and Control (CDC)*, pages 1032–1037, 2020. doi: 10.1109/CDC42340.2020.9304340.
- [92] Cacace, Simone, Camilli, Fabio, and Goffi, Alessandro. A policy iteration method for mean field games. *ESAIM: COCV*, 27:85, 2021. doi: 10.1051/cocv/2021081. URL <https://doi.org/10.1051/cocv/2021081>.
- [93] Julien Pérolat, Sarah Perrin, Romuald Elie, Mathieu Laurière, Georgios Piliouras, Matthieu Geist, Karl Tuyls, and Olivier Pietquin. Scaling up Mean Field Games with Online Mirror Descent, 2021.
- [94] Dario Bauso, Hamidou Tembine, and Tamer Başar. Robust mean field games. *Dynamic games and applications*, 6(3):277–303, 2016.
- [95] Jun Moon and Tamer Başar. Linear Quadratic Risk-Sensitive and Robust Mean Field Games. *IEEE Transactions on Automatic Control*, 62(3):1062–1077, 2017. doi: 10.1109/TAC.2016.2579264.
- [96] Jianhui Huang and Minyi Huang. Robust Mean Field Linear-Quadratic-Gaussian Games with Unknown L^2 -Disturbance. *SIAM Journal on Control and Optimization*, 55(5):2811–2840, 2017. doi: 10.1137/15M1014437. URL <https://doi.org/10.1137/15M1014437>.
- [97] Chungang Yang, Haoxiang Dai, Jiandong Li, Yue Zhang, and Zhu Han. Distributed Interference-Aware Power Control in Ultra-Dense Small Cell Networks: A Robust Mean Field Game. *IEEE Access*, 6:12608–12619, 2018. doi: 10.1109/ACCESS.2018.2799138.
- [98] Amoolya Tirumalai and John S. Baras. A Robust Mean-field Game of Boltzmann-Vlasov-like Traffic Flow. In *2022 American Control Conference (ACC)*, pages 556–561, 2022. doi: 10.23919/ACC53348.2022.9867331.
- [99] A. E. Eiben and J. E. Smith. *What Is an Evolutionary Algorithm?*, pages 25–48. Springer Berlin Heidelberg, Berlin, Heidelberg, 2015. ISBN 978-3-662-44874-8. doi: 10.1007/978-3-662-44874-8_3. URL https://doi.org/10.1007/978-3-662-44874-8_3.
- [100] Nicolas Cambier, Vincent Frémont, Vito Trianni, and Eliseo Ferrante. Embodied Evolution of Self-organised Aggregation by Cultural Propagation. In Marco Dorigo, Mauro Birattari, Christian Blum, Anders L. Christensen, Andreagiovanni Reina, and Vito Trianni, editors, *Swarm Intelligence*, pages 351–359, Cham, 2018. Springer International Publishing. ISBN 978-3-030-00533-7.
- [101] Ahmed Touati, Amy Zhang, Joelle Pineau, and Pascal Vincent. Stable Policy Optimization via Off-Policy Divergence Regularization. In *Conference on Uncertainty in Artificial Intelligence*, pages 1328–1337. PMLR, 2020.

- [102] Xin Guo, Renyuan Xu, and Thaleia Zariphopoulou. Entropy Regularization for Mean Field Games with Learning. *Math. Oper. Res.*, 47(4):3239–3260, nov 2022. ISSN 0364-765X. doi: 10.1287/moor.2021.1238. URL <https://doi.org/10.1287/moor.2021.1238>.
- [103] Kefan Su and Zongqing Lu. Divergence-Regularized Multi-Agent Actor-Critic. In Kamalika Chaudhuri, Stefanie Jegelka, Le Song, Csaba Szepesvari, Gang Niu, and Sivan Sabato, editors, *Proceedings of the 39th International Conference on Machine Learning*, volume 162 of *Proceedings of Machine Learning Research*, pages 20580–20603. PMLR, 17–23 Jul 2022. URL <https://proceedings.mlr.press/v162/su22b.html>.
- [104] Yaodong Yang, Rui Luo, Minne Li, Ming Zhou, Weinan Zhang, and Jun Wang. Mean Field Multi-Agent Reinforcement Learning. In Jennifer Dy and Andreas Krause, editors, *Proceedings of the 35th International Conference on Machine Learning*, volume 80 of *Proceedings of Machine Learning Research*, pages 5571–5580. PMLR, 10–15 Jul 2018. URL <https://proceedings.mlr.press/v80/yang18d.html>.
- [105] Sriram Ganapathi Subramanian, Matthew E. Taylor, Mark Crowley, and Pascal Poupart. Partially Observable Mean Field Reinforcement Learning, 2020. URL <https://arxiv.org/abs/2012.15791>.
- [106] Sriram Ganapathi Subramanian, Pascal Poupart, Matthew E. Taylor, and Nidhi Hegde. Multi Type Mean Field Reinforcement Learning, 2022.
- [107] Sriram Ganapathi Subramanian, Matthew E. Taylor, Mark Crowley, and Pascal Poupart. Decentralized Mean Field Games, 2021. URL <https://arxiv.org/abs/2112.09099>.
- [108] Sarah Perrin, Mathieu Laurière, Julien Pérolat, Romuald Élie, Matthieu Geist, and Olivier Pietquin. Generalization in mean field games by learning master policies. In *Proceedings of the AAAI Conference on Artificial Intelligence*, volume 36, pages 9413–9421, 2022.
- [109] René Carmona, Mathieu Laurière, and Zongjun Tan. Model-Free Mean-Field Reinforcement Learning: Mean-Field MDP and Mean-Field Q-Learning, 2021.
- [110] Sharan Vaswani, Olivier Bachem, Simone Totaro, Robert Mueller, Matthieu Geist, Marlos C. Machado, Pablo Samuel Castro, and Nicolas Le Roux. A functional mirror ascent view of policy gradient methods with function approximation. *CoRR*, abs/2108.05828, 2021. URL <https://arxiv.org/abs/2108.05828>.
- [111] Shangdong Zhang and Richard S Sutton. A deeper look at experience replay. *arXiv preprint arXiv:1712.01275*, 2017.

Appendix to ‘Networked Communication for Decentralised Agents in Mean-Field Games’

A Extended related work

As we emphasise in Section 1, the MFG framework was originally mainly theoretical, and our work continues in the vein of those seeking to increase its practical applicability [38; 39; 88]. In early works, the MFE was found by solving a coupled system of dynamical equations: a forward evolution equation for the mean-field distribution, and a backwards equation for the representative agent’s optimal response to the mean-field distribution; crucially, these methods relied on the assumption of an infinite population [45]. Early work solved the coupled equations using numerical methods that did not scale well for more complex state and action spaces [46–49]; or, even if they could handle higher-dimensional problems, the methods were based on known models of the environment’s dynamics [41; 51; 63–66], and/or computed a best-response to the mean-field distribution [19; 20; 39; 45; 51; 52; 62; 67]. The latter approach is both computationally inefficient in non-trivial settings [43; 45], and in many cases is not convergent (as in general it does not induce a contractive operator) [19; 90]. Subsequent work has therefore moved towards model-free and/or policy-improvement scenarios [37; 45; 50; 53; 54; 91–93], possibly with learning taking place by observing N -agent *empirical* population distributions [43; 73].

Most prior works, including algorithms designed to solve the MFG using an N -agent empirical distribution, have also assumed an oracle that can generate samples of the game dynamics (for any distribution) to be provided to the learning agent [41; 50; 51], or otherwise that the algorithm has direct control over the population distribution at each time step, such as in cases when the agents’ policies and distribution are updated on different timescales, with the *fictitious play* method being particularly popular [19–21; 35; 42; 52–60]. In practice, many-agent problems may not admit such arbitrary generation or manipulation (for example, in the context of robotics or controlling vehicle traffic), and so a desirable quality of learning algorithms is that they control only the agents’ behavioural policies, rather than their states. Learning may also need to leverage continuing, rather than episodic, tasks [3]. Yongacoglu et al. [73] and Yardim et al. [43] therefore present algorithms that seek the MFE using only a single evolution of the empirical population. Almost all prior work relies on a centralised controller to conduct learning on behalf of all the agents [21; 41; 42; 45; 68]. More recent work has explored MFG algorithms for independent learning with N agents [43; 60; 73; 74].

Naturally, inter-agent communication is more applicable in settings where learning takes place along a single path, rather than the distribution being arbitrarily reset for new episodes, and the distribution is not manipulated by an oracle, since these imply a level of external control over the population that results in centralised learning. Equally, it is in situations of learning from real, deployed agents (rather than simulated settings) that we are most likely to be concerned with fault tolerance. As such, our work is most closely related to Yardim et al. [43] and Yongacoglu et al. [73], which provide algorithms for centralised and independent learning with empirical distributions along continued system evolution paths: we contribute a networked learning algorithm in this setting. Yongacoglu et al. [73] empirically demonstrates an independent learning algorithm when agents observe compressed information about the mean-field distribution as well as their local state, but they do not compare this to any other algorithms or baselines. Yardim et al. [43] compares algorithms for centralised and independent learning theoretically, but does not provide empirical demonstrations. In contrast, we empirically demonstrate our networked learning algorithm, where agents observe only their local state, in comparison to both centralised and independent baselines, as well as analysing their sample complexity theoretically.

An existing area of work called ‘robust mean-field games’ studies the robustness of these games to uncertainty in their transition and reward functions [36; 75; 94–98]. We inherently consider this uncertainty via our model-free learning, and instead focus on robustness to failures and changes in the agent population itself.

We note a similarity between 1. our method for deciding which policies to propagate through the population (described in Section 3.3) and 2. the computation of evaluation/fitness functions within evolutionary algorithms to indicate which solutions are desirable to keep in the population for the next generation [99]. Works such as Cambier et al. [100] have also demonstrated the combination

of evolutionary approaches and multi-agent communication for self-organised behaviours in swarm robotics.

B Extended discussion of application of communication networks to MFGs

We consider in particular two scenarios to which we desire real-world many-agent systems to be robust; these form the basis for our robustness experiments. The networked setup affords the population fault-tolerance and online scalability, which are motivating qualities of many-agent systems in the first place.

Firstly, we consider a scenario in which the learning/updating procedure of agents fails with a certain probability within each iteration. In decentralised settings, this might be particularly liable to occur since the updating process might only be synchronised between agents by internal clock ticks, such that some agents may not complete their update in the allotted time but will nevertheless be required to take the next step in the environment. Such failures slow the improvement of the population in the independent case, and in the centralised setting it means no improvement occurs at all in any iteration in which failure occurs (the single point of failure). Networked communication provides redundancy in the case of failure, with the updated policies of any agents that have managed to learn spreading through the population to those that have not. This ensures that improvement can continue for the whole population even if a high number of agents do not manage to learn independently in a given iteration.

Secondly, we may want to arbitrarily increase the size of a population of agents that are already learning or operating in the environment (we can imagine extra fleets of autonomous cars or drones being deployed). A purely independent setting would require all the new agents to learn a policy individually given the existing distribution, and the process of their following and improving policies from scratch may itself disturb the Nash equilibrium that has already been achieved by the original population. With a communication network, however, the policy (or, if there is not unanimous consensus at that point, policies) that has been learnt so far can quickly be shared with the new agents in a decentralised way, hopefully before their unoptimised policies can destabilise the current Nash equilibrium. This would provide, for example, a way to bootstrap a large population from a smaller pre-trained group, if training were considered expensive in a given setting.

We preempt objections that communication with neighbours might violate the anonymity that is characteristic of the mean-field paradigm, by emphasising that the communication in our algorithm takes place outside of the ongoing learning-and-updating parts of each iteration. Thus the core learning assumptions of the mean-field paradigm are unaffected, as they essentially apply at a different level of abstraction (a convenient approximation) to the reality we face of N agents that interact within the same environment. Indeed, prior works have combined networks with mean-field theory, such as using a mean field to describe adaptive dynamical networks [40].

C Properties of policy adoption via communication over the network (extended discussion)

Agents generate σ_{k+1}^i as $\|\pi_{k+1}^i - \pi_k^i\|_1$ (the number gets communicated through the network with the associated policy, it does not get recomputed by each agent). This means that policies that proliferate through the population are ones that differ the least from their ancestors. This does not guarantee that policies remaining after C will be the closest to each other of all possible combinations of policies that existed before C , but absent the ability to make such comparisons between policies across parts of the communication network that by definition lack (direct, or perhaps even indirect,) connection, our method reduces the likely divergence by reducing the distance to a common reference point.

Even if unanimous consensus is not achieved in the population during C rounds for several consecutive iterations of the k loop, all policies ultimately have a common ancestor in Line 1; minimising the divergence from any common ancestor minimises the likely divergence among the descendants. (In reality, the mixing of the population due to entropy-regularised policies makes it unlikely that pockets of the population would remain isolated with distinct policies for several iterations of the k loop, assuming the network depends on the agents' locations.)

Deciding between policies by selecting those that differ little from their ancestors also has a secondary benefit, by serving similarly to minimising the learning rate η in Definition 3.2. This stabilises learning and policy improvement, avoiding large changes in policy and hence the population distribution [101].

There is a small possibility that two distinct policies may generate the same similarity metric, such that agents need to break a tie in order to agree on a policy. If considered necessary in practice, we could resolve this issue by computing a secondary similarity metric to be broadcast alongside the first, such as the following: $\|\pi - \pi'\|_{tot} := \sum_{s \in \mathcal{S}} \|\pi(s) - \pi'(s)\|_1$. In the even more unlikely scenario that these metrics are also the same for two distinct policies, agents could broadcast a unique ID number so as to break ties arbitrarily.

D Proofs

D.1 Proof of Theorem 3.1

Proof. For distinct policies π_{k+1}^i and π_{k+1}^j , $\|\pi_{k+1}^i - \pi_{k+1}^j\|_1 > 0$. If agent j adopts π_{k+1}^i then $\pi_{k+1}^i = \pi_{k+1}^j$ such that $\|\pi_{k+1}^i - \pi_{k+1}^j\|_1 = 0$. If we take $\bar{\pi} = \pi_{k+1}^i$, then we have reduced $\Delta_{\bar{\pi}} := \frac{1}{N} \sum_i \|\bar{\pi} - \pi^i\|_1$. \square

D.2 Proof of Theorem 3.2

Proof. Let us form a sphere with centre π_k and radius $\max_{\psi \in \Psi} \|\psi - \pi_k\|_1$. By definition, all the policies in Ψ fall within this sphere, such that $\forall a, b \in \Psi, \|a - b\|_1 \leq \max_{\psi \in \Psi} 2\|\psi - \pi_k\|_1$. By including in Ψ policies π_{k+1}^i that minimise $\|\pi_{k+1}^i - \pi_k\|_1$, we inherently also minimise $\max_{\psi \in \Psi} 2\|\psi - \pi_k\|_1$. While this does not guarantee that Ψ contains the policies given by $\min_{i, j \in \{1, \dots, N\}} \|\pi_{k+1}^i - \pi_{k+1}^j\|_1$, we have nevertheless used the information available to us to reduce the bound on $\|a - b\|_1 \forall a, b \in \Psi$. \square

D.3 Proof of Theorem 3.3

It can be helpful to consider that our networked architecture is effectively a generalisation of the centralised and independent settings. The independent setting is the special case of the networked algorithm where none of the agents have links between them for any of an arbitrary number of communication rounds. The centralised setting is the special case when the method for generating σ_{k+1}^i involves a unique ID for each agent rather than the similarity metric in Line 11 of Algorithm 1, with the central learner being assumed to generate the lowest value by default, and the number of sharing rounds assumed to be large enough that the central learner's policy is always adopted by the entire population.

Proof. Call agent ω_k the agent which, after the PMA update at iteration k , has the policy furthest from π^* such that $\omega_k = \arg \max_{x \in \{i, \dots, N\}} \|\pi_k^x - \pi^*\|_1$. Suppose firstly that \mathcal{G}_t has no connections between any agents for any t , such that no communication ever takes place. Since this reflects the independent learning setting, by Theorem 3 in Yardim et al. [43], we know that despite ω_k being the 'worst performing' agent, it nevertheless respects

$$\mathbb{E}[\|\pi_K^{\omega_K} - \pi^*\|_1] \leq \epsilon + \frac{\chi}{\sqrt{N}}.$$

Call the policy divergence in this setting $\Delta_{\bar{\pi}_k}^{ind}$. Now suppose instead that \mathcal{G}_t does contain some communication links for some t during the algorithm's communication rounds, such that policy communication and adoption does occur for some k . Suppose also that only the worst performing ω_k ever has its policy adopted by others. If we call the policy divergence in this setting $\Delta_{\bar{\pi}_k}^{net}$, then by Theorems 3.1 and 3.2, $\Delta_{\bar{\pi}_k}^{net} \leq \Delta_{\bar{\pi}_k}^{ind} \forall k$. Since the bias in the empirical distribution and therefore also in value estimation has been reduced, the iteration complexity will be improved, such that $\forall j$

$$\mathbb{E}[\|\pi_K^{j, net} - \pi^*\|_1] \leq \mathbb{E}[\|\pi_K^{\omega_K} - \pi^*\|_1].$$

In reality, we can expect our algorithm to reduce $\Delta_{\bar{\pi}_k}^{net}$ drastically across many k due to the joint connectedness of sequences of \mathcal{G}_t , often such that $\Delta_{\bar{\pi}_k}^{net} = 0$. It is therefore likely that the sample complexity of our algorithm will significantly outperform that of the independent algorithm. \square

E Algorithm acceleration by use of experience-replay buffer (further details)

Algorithm 2 Networked learning with experience replay

Require: loop parameters $K, M_{pg}, M_{td}, C, W, L$, learning parameters $\eta, \beta, \lambda, \gamma$

Require: initial states $\{s_0^i\}_i$

```

1: Set  $\pi_0^i = \pi_{max}, \forall i$  and  $t \leftarrow 0$ 
2: for  $k = 0, \dots, K - 1$  do
3:    $\forall s, a, i : \hat{Q}_0^i(s, a) = Q_{max}$ 
4:    $\forall i$ : Empty  $i$ 's buffer
5:   for  $m = 0, \dots, M_{pg} - 1$  do
6:     for  $M_{td}$  iterations do
7:       Take step  $\forall i : a_t^i \sim \pi_k^i(\cdot | s_t^i), r_t^i = R(s_t^i, a_t^i, \hat{\mu}_t), s_{t+1}^i \sim P(\cdot | s_t^i, a_t^i, \hat{\mu}_t)$ 
8:        $t \leftarrow t + 1$ 
9:     end for
10:    if  $m > W$  then
11:       $\forall i$ : Add  $\zeta_{t-2}^i$  to  $i$ 's buffer
12:    end if
13:  end for
14:  for  $l = 0, \dots, L - 1$  do
15:     $\forall i$ : Shuffle buffer
16:    for transition  $\zeta_l^i$  in  $i$ 's buffer do ( $\forall i$ )
17:      Compute TD update ( $\forall i$ ):  $\hat{Q}_{m+1}^i = \tilde{F}^{\pi_k^i}(\hat{Q}_m^i, \zeta_{t-2}^i, \beta)$  (see Definition 3.1)
18:    end for
19:  end for
20:  PMA step  $\forall i : \pi_{k+1}^i = \Gamma_\eta^{md}(\hat{Q}_L^i, \pi_k^i)$  (see Definition 3.2)
21:   $\forall i : \sigma_{k+1}^i = \|\pi_{k+1}^i - \pi_k^i\|_1$ 
22:  for  $C$  rounds do
23:     $\forall i$ : Broadcast  $\sigma_{k+1}^i, \pi_{k+1}^i$ 
24:     $\forall i : J_t^i = \{j \in \mathcal{N} : (i, j) \in \mathcal{E}_t\}$ 
25:     $\forall i$ : chosen $^i = \arg \min_{x \in \{i \cup J_t^i\}} \sigma_{k+1}^x$ 
26:     $\forall i : \sigma_{k+1}^i = \sigma_{k+1}^{chosen^i}, \pi_{k+1}^i = \pi_{k+1}^{chosen^i}$ 
27:    Take step  $\forall i : a_t^i \sim \pi_{k+1}^i(\cdot | s_t^i), r_t^i = R(s_t^i, a_t^i, \hat{\mu}_t), s_{t+1}^i \sim P(\cdot | s_t^i, a_t^i, \hat{\mu}_t)$ 
28:     $t \leftarrow t + 1$ 
29:  end for
30: end for
31: Return policies  $\{\pi_K^i\}_i$ 

```

Our theoretical analysis of online learning from a single system evolution path relies on mixing assumptions [43, Assumptions 3,4]. Excitation and mixing constants given in these assumptions lead to very small learning rates $\{\beta_m\}_{m \in \{0, \dots, M_{pg}-1\}}$ ([43, Theorem 1]), which in turn results in a number of TD updates - and hence iterations of the M_{pg} loop (Line 4, Algorithm 1) - that is very large. For one of our experimental environments, for example, we calculated that M_{pg} would need to be of the order **e+17**, even in the centralised case. Recall additionally that, within each M_{pg} iteration, there is also an inner loop of M_{td} iterations (Line 5, Algorithm 1), which can further increase by several orders of magnitude the total number of environment steps required. Overall, these requirements, which are derived from the theoretical bounds, render the algorithm's convergence impractically slow.

The intuition behind the better learning efficiency resulting from our experience replay buffer in Algorithm 2 is as follows. The value of a state-action pair p is dependent on the values of subsequent states reached, but the value of p is only updated when the TD update is conducted on p , rather than every time a subsequent pair is updated. By learning from each stored transition multiple times, we

not only make repeated use of the reward and transition information in each costly experience, but also repeatedly update each state-action pair in light of its likewise updated subsequent states.

The transitions in the buffer are discarded after the replay cycles and a new buffer is initialised for the next iteration k , as in Line 4. As such the space complexity of the buffer only grows linearly with the number of M_{pg} iterations within each outer loop k , rather than with the number of K loops.

F Experiments

Experiments were conducted on a MacBook Pro, Apple M1 Max chip, 32 GB, 10 cores. We used multiprocessing for the learning and policy update sections of our code.

F.1 Tasks

We conduct numerical tests with three games (defined by the agents’ objectives), chosen for being particularly amenable to intuitive and visualisable understanding of whether the agents are learning behaviours that are appropriate and explainable for the respective objective functions. In all cases, rewards are normalised in $[0,1]$ after they are computed. In experiments involving targets, we place one target in each of the four corners of the grid.

Cluster (not included in main text). This is the inverse of the ‘exploration’ game in Laurière et al. [19], where now agents are encouraged to gather together by the reward function $R(s_t^i, a_t^i, \hat{\mu}_t) = \log(\hat{\mu}_t(s_t^i))$. That is, agent i receives a reward that is logarithmically proportional to the fraction of the population that is co-located with it at time t . We give the population no indication where they should cluster, agreeing this themselves over time.

Agree on a single target. Unlike in the above ‘cluster’ game, the agents are given options of locations to gather at, and they must reach consensus among themselves. If the agents are co-located with one of a number of specified targets $\tau \in T$, and other agents are also at that target, they get a reward proportional to the fraction of the population found there; otherwise they receive a penalty of -1. In other words, the agents must cooperate on which of a number of mutually beneficial points will be their single gathering place. The reward function is given by $R(s_t^i, a_t^i, \hat{\mu}_t) = r_{targ}(r_{collab}(\hat{\mu}_t(s_t^i)))$, where

$$r_{targ}(x) = \begin{cases} x & \text{if } \exists \tau \in T \text{ s.t. } \text{dist}(s_t^i, \tau) = 0 \\ -1 & \text{otherwise,} \end{cases} \quad r_{collab}(x) = \begin{cases} x & \text{if } \hat{\mu}_t(s_t^i) > 1/N \\ -1 & \text{otherwise.} \end{cases}$$

Diffuse across multiple targets. Similar to the ‘crowd modelling with congestion’ game in [19; 67], the agents seek out one of a number of targets $\tau \in T$, while avoiding crowds at the target, such that the targets should receive equal coverage from the population. The reward function is given by $R(s_t^i, a_t^i, \hat{\mu}_t) = r_{targ}(r_{averse}(\hat{\mu}_t(s_t^i)))$, where $r_{targ}(x)$ is as above and $r_{averse}(\hat{\mu}_t(s_t^i)) = \text{gridDimension} + 1 - \hat{\mu}_t(s_t^i)$. The constant ‘gridDimension + 1’ is provided to incentivise agents to move to another more sparsely populated target despite the penalty of -1 incurred for every step away from a target.

F.2 Exploitability

Works on MFGs frequently use the *exploitability* metric to evaluate how close a given policy π is to a Nash equilibrium policy π^* [19; 20; 45; 67; 89]. The metric quantifies how much an agent can benefit by deviating from the policy pursued by the rest of the population, by measuring the difference between the return given by a policy that maximises the expected discounted regularised (via h) reward V_h for a given population distribution, and the return given by the policy that gives rise to this distribution. If π has a large exploitability then an agent can significantly improve its return by deviating from π , meaning that π is far from π^* , whereas an exploitability of 0 implies that $\pi = \pi^*$. Denote by μ^π the distribution generated when π is the policy followed by all of the population aside from the deviating agent; then the exploitability of policy π is defined as:

$$\mathcal{E}(\pi) = \max_{\pi'} V_h(\pi', \mu^\pi) - V_h(\pi, \mu^\pi).$$

Since we do not have access to the exact best response policy $\arg \max_{\pi'} V_h(\pi', \mu^\pi)$, we instead approximate the exploitability metric, similarly to Perrin et al. [52], as follows. We freeze the policy of all agents apart from a deviating agent, for which we store its current policy and then conduct three k iterations of policy improvement. Then, to approximate the expectations, we take the mean discounted regularised reward for the deviating agent across a separate three k loops, as well as the mean of all the other agents’ returns across these same three loops. We then revert the agent back to its stored policy, before learning continues for all agents. As such, the quality of our approximation is limited by the number of rounds of both improvement and testing, which must be restricted for the sake of running speed of the experiments; for this reason the metric appears noisy in our results.

Since prior works conducting empirical testing have generally focused on the centralised setting, evaluations have not had to consider the exploitability metric when not all agents are following a single policy π , as may occur in the the independent or networked settings. The method described above for approximating exploitability involves calculating the mean return of all non-deviating agents’ policies. While this is π in the centralised case, if the non-deviating agents do not share a single policy, then this method is in fact approximating the exploitability of their joint policy π^{-d} , where d is the deviating agent. Measuring the performance of the joint policy can suggest that the population has found an adequate solution to the problem even when it is in fact far from the mean-field Nash equilibrium, since the agents may not be close to sharing a single well-performing policy. Any one of the individual policies that make up the joint policy may lead to high exploitability if all agents were to follow this policy rather than the joint policy. For further discussion of the issues with this, see Section F.3.

A better metric, in this case, could therefore be the average exploitability of the independent policies within the joint policy:

$$\mathcal{E}(\pi^{-d}) = \frac{1}{N-1} \sum_i^{N-1} \left[\max_{\pi'} V_h(\pi', \mu^{\pi^i}) - V_h(\pi^i, \mu^{\pi^i}) \right].$$

To compute this would require copying a policy π^i in π^{-d} to all the other non-deviating agents (storing their prior policies), and approximating the exploitability of π^i by the method described above for π , and then restoring their prior policies and repeating this process for all the other i . However, aside from undermining the premise of the decentralised architecture by arbitrarily copying policies to all of the agents, computing such a metric would also prohibitively slow our experiments by drastically increasing the number of loops required. For this reason, we use several proxy metrics in our experiments, rather than this single idealised metric.

F.3 Divergent policies

In our experiments, the joint policy π^{-d} in the independent case often appears to reach similar exploitability and mean regularised return to π in the centralised case. However, this can be misleading, as it does not actually mean that the individual policies within π^{-d} are getting closer to a single Nash equilibrium policy π^* . We can see this in our plots in Section 4 and Appendix F.5, where the independent architecture gives joint policies of which the exploitability and mean return appear to converge, despite the difference between the individual policies increasing. Each of the individual policies that make up the joint policy may lead to high exploitability and low return if all agents were to follow this policy rather than the joint policy, meaning that this is a superficially high-performing but possibly undesirable solution.

There are numerous reasons why this might be a problem when applied to real-world systems. Equilibria composed of heterogeneous policies are likely harder to analyse, with negative impacts on interpretability and safety assurance. They may also have adverse consequences with respect to the robustness desiderata we have for deployed systems, as follows. Independent agents that appear to perform well with divergent policies do so based on the current combination of diverse policies that make up the joint policy [73]. If one or more agents, of which the combined policies were crucial to the success of the overall joint policy, were to happen to leave the population for some reason at a similar time, the lack of redundancy might mean that the whole population distribution changes and the equilibrium is disturbed, whereas this risk does not occur when all agents share a common policy and can therefore be substituted for each other. For example, in the ‘diffuse across all targets’ game, the population receives the highest reward when it is equally spread across the targets in each of the four corners of the grid. If the agents at one corner happened to stop functioning at a given moment,

then if the population had a common policy for covering all of the targets it would likely quickly redistribute itself without much disruption. When agents have divergent policies, a different quarter of the population may simply learn to remain at each corner. This means that if such a malfunction were to occur, the agents may not redistribute at all (due to insufficient exploration), or, if they did attempt to, it could throw off the existing equilibrium, with agents needing to learn entirely new policies and protractedly upsetting the distribution while they did so.

F.4 Hyperparameters

Please see Table 1 for our hyperparameter choices. We can group our hyperparameters into those controlling the number of iterations of each loop in the algorithm (considerations regarding which we have discussed in Section 3.5 and Appendix E), and those affecting the learning or policy updates ($\eta, \beta, \lambda, \gamma$). Care must be taken when selecting a practical policy update rate η , as we found that both this and the method for generating σ_{k+1}^i can affect learning stability.

Also of particular note is the choice of the entropy regularisation scaling hyperparameter λ (Section 2). As in some earlier works [41; 43; 67; 90; 102], our algorithms employ regularisation to ensure theoretical convergence. However, it has been recognised that modifying the RL objective in this way can bias the Nash equilibrium [19; 43; 103]. Therefore, when using the entropy regulariser for practical implementation of these algorithms, it is important to consider an appropriate choice of λ to ensure that the resulting equilibrium truly reflects the goal behaviour that the designer was intending for the population. For example, if λ is not small in our grid-world environment, the population (which is initialised with maximum entropy policies) finds itself from the start at a unique stable equilibrium where all agents constantly move around the environment at random, regardless of whether the intended objective was to cluster in one place (the way to be close to agents that are moving around with high entropy is also to move around with high entropy) or to disperse to unoccupied regions (if all regions are occupied with high entropy, one should also continue moving with high entropy). One may therefore have to trade off speed of convergence to a unique equilibrium with how faithfully the resulting distribution fulfils the desired underlying task.

In our experiments, we set λ as 0.01. Larger values led to the problems described above; it may be the case that in our environments convergence would have been achieved equally fast with λ at or closer to 0, but we did not determine this conclusively.

F.5 Additional experiments

We include here the results for the ‘cluster’ task. Due to the greater number of k iterations required for convergence in this task, we changed two of our other hyperparameters (from those given in Table 1 for the other experiments) in order to speed up the experiment runtime. For the experiment in Figure 5 we used a population of 50 agents instead of 200. For the experiment in Figure 6 the population begins at 50 agents and increases to 100 (rather than jumping from 25 to 200). For this latter experiment we also conducted 4 trials of each algorithm, rather than 10.

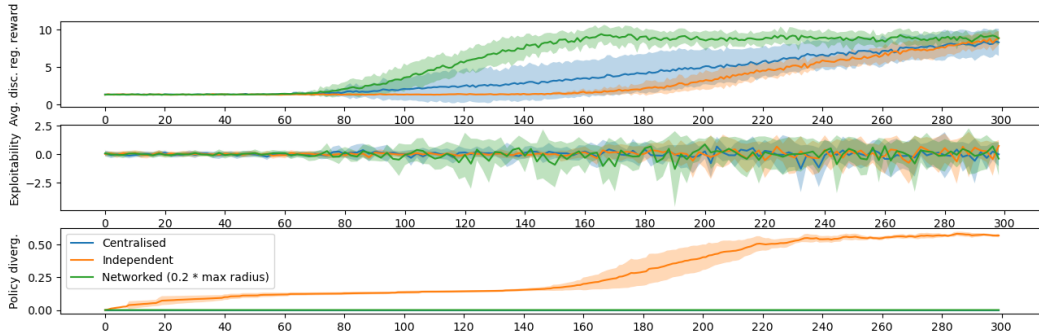


Figure 5: Cluster - 50% chance of learning failure at every iteration.

Our networked algorithm outperforms the others in similar ways to the results of the experiments for the other tasks, as discussed in Section 4.2. Of particular note is that we observed no increase

Table 1: Hyperparameters

Hyperparameter	Value	Comment
Trials	10/algorithm	We report the mean and standard deviation of each metric across the trials.
Population	200	We ran tests with the number of agents ranging between 10 and 300, with the algorithms performing equally well with all population sizes, apart from in the ‘cluster’ task (see Appendix F.5). We chose 200 for our demonstrations displayed in the main text, to show our algorithm’s applicability to large-scale systems. For further discussion, see Section G. In experiments testing robustness to one-time population increases, the population instead begins at 25 agents and has 175 added at the marked time point (apart from in the ‘cluster’ task).
Gridsize	8x8	Any other grid sizes are of course possible, but the 8x8 one is deemed large enough to showcase that agents were learning suitable policies, rather than finding their targets by chance.
Communication radius	0.2 * grid diagonal	We can conduct further experiments to show the effect of neighbourhood size on performance of our algorithm.
γ	0.9	Standard choice across RL literature.
K	Varies	K is chosen such that we can see the discounted return converging.
M_{pg}	3000	We tested M_{pg} in {1000,1500,2000,2500,10000}. In combination with our other hyperparameters, we found $M_{pg} < 3000$ did not lead to good results, possibly due to the combination of $ \mathcal{S} \mathcal{A} = 320$ with learning rate $\beta = 0.1$.
M_{td}	10	We tested M_{pg} in {1,2,10,100}. We found that the networked algorithm received notably lower discounted return than the centralised algorithm when $M_{td} < 10$.
β	0.1	We tested β in {0.01,0.1} and found 0.1 to be small enough for sufficient learning at an acceptable speed. Further optimising this hyperparameter (including by having it decrease with increasing $l \in L$) may lead to better results.
L	500	We tested L in {300,400,500}. In combination with our other hyperparameters, we found $L < 500$ did not lead to good results.
η	0.01	We tested η in {0.001,0.01,0.1,1,10} and found that 0.01 gave reasonably stable learning that progressed sufficiently quickly. Further optimising this hyperparameter may lead to better results.
λ	0.01	We tested λ in {0,0.0001,0.001,0.01,0.1,1}. For further discussion, see Section F.4.
W	20	We include this hyperparameter to ensure that the population settles to the new empirical distribution after a policy update before learning resumes. An appropriate choice for this value is therefore likely to rely particularly on the other waiting hyperparameter M_{td} , and also on λ and η (which affect how quickly the new distribution is reached), as well as M_{pg} , L and β , which may affect the relative impact on learning of any transitions that are added to the buffer before the new distribution is stable. We found that a choice of 20 gave sufficient results, but further experimentation is required to understand whether this parameter can be optimised with respect to the other hyperparameters.
C	300	This is large enough to ensure unanimous policy consensus for almost every iteration k in our setting. In fact, it may be possible to have C significantly lower and still achieve similar results.

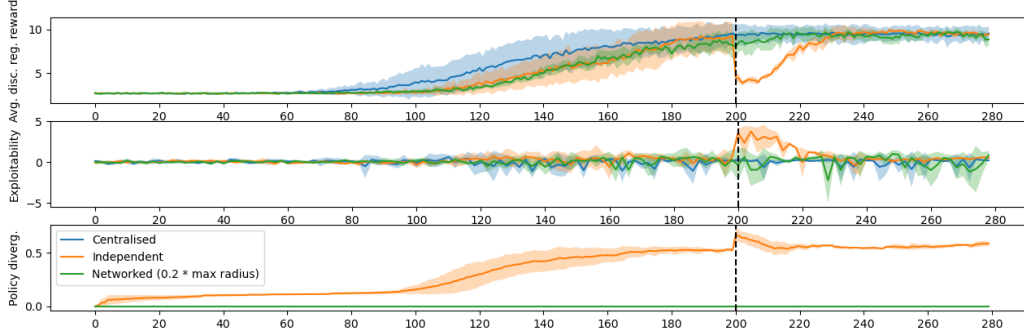


Figure 6: Cluster - the population increases from 50 to 100 agents at iteration 200.

in the average return on this task when the population size was set at 25 in an initial test (plot not shown here), whereas there was convergence when $N = 50$, reflecting the fact that the empirical distribution approximates the mean field better for greater N , as in Theorem 3.3. We did not observe such sensitivity in the other games; this is likely because in our ‘cluster’ game the agents’ rewards depend entirely on the population distribution and not on the proximity to specified targets, increasing the importance of a well-approximated mean-field distribution. Future work will involve further studying the effect of population size on practical convergence to the Nash equilibrium, especially in interaction with the type of task and the other hyperparameter choices.

G Limitations and ongoing work

Our incorporation of the experience-replay buffer (Section 3.5) allows us to increase the convergence speed of our algorithms to a reasonable number of steps k , despite reducing values of M_{pg} and M_{td} . Nevertheless, our experiments can still take a significant amount of time to run: experiments involving 10 runs of each of the three algorithms with 200 agents required several hundred CPU hours (~ 400 CPU hours for $K = 150$). However, we believe this to be related to the nature of the experimental process rather than necessarily indicative of issues with the applicability to real-world problems, as we explain in the following. Our experiments take longer to run as the size of the population N grows (albeit only linearly), due to the need to manage the action step and learning process of each agent synchronously, even when simulating their decentralised behaviour. We found that reducing the size N of our test population speeds up experiments while usually not affecting our results, but we selected N as 200 for most experiments to show that our algorithm can handle large populations, indeed often larger than those demonstrated in other mean-field works, especially for grid-world environments [50; 53; 73; 88; 90; 104–107]. Multiprocessing can mitigate this bottleneck only slightly, due to limited processors and context-switching overheads. Nevertheless, our experiments are only meant to provide empirical demonstration of the benefits of our algorithm, which in reality is intended to be implemented on populations of decentralised agents learning and acting individually: in such cases, all execution and updating steps would be asynchronous, hence the number of agents would have negligible effect on the time to complete each step of the algorithm.

As described in Section F.2, to approximate the exploitability metric we run six extra k iterations (three for policy improvement of the deviating agent, three for policy evaluation) for every two k iterations that are part of the actual training procedure. Reducing these computations in deployed settings, or relying on other performance metrics, would also significantly speed up runtime.

A natural continuation of our work is to introduce communication networks to MFGs with non-stationary equilibria. A promising method for such games is to have agents’ policies depend both on their local state and also on the population distribution [45; 91; 108; 109], but such a high-dimensional observation object is likely to require moving beyond tabular settings. Both for this reason, and in order to handle larger and continuous state/action spaces, ongoing work involves extending our new framework to handle function approximation, which includes modifying the PMA step for this purpose [110]. In these settings, agents will communicate the parameters of their policy functions,

which could be approximated. Our experience-replay buffer will be helpful in providing uncorrelated data to train the function approximators [111].

Naturally, it may be a strong assumption to suppose that decentralised agents with local state observations and limited communication radius would be able to observe the entire population distribution. We can therefore explore a framework of agents estimating the empirical distribution from only their local neighbourhood as in Subramanian et al. [105], and possibly also improving this estimation by communicating with neighbours [73], such that this useful information spreads through the network along with policy parameters. In both this extended setting and our existing architecture, it is worth experimenting further with the selection of the communication radius in combination with the number of communication rounds, and their effect on the performance of networked populations.